

Titre: Design and Validation of a Hydrogen Peroxide Vapour
Title: Decontamination System

Auteur: Mathieu Chartray-Pronovost
Author:

Date: 2022

Type: Mémoire ou thèse / Dissertation or Thesis

Référence: Chartray-Pronovost, M. (2022). Design and Validation of a Hydrogen Peroxide
Citation: Vapour Decontamination System [Master's thesis, Polytechnique Montréal].
PolyPublie. <https://publications.polymtl.ca/10505/>

 **Document en libre accès dans PolyPublie**
Open Access document in PolyPublie

URL de PolyPublie: <https://publications.polymtl.ca/10505/>
PolyPublie URL:

**Directeurs de
recherche:** Étienne Robert
Advisors:

Programme: Génie aérospatial
Program:

POLYTECHNIQUE MONTRÉAL
affiliée à l'Université de Montréal

Design and Validation of a Hydrogen Peroxide Vapour Decontamination System

MATHIEU CHARTRAY-PRONOVOST
Département de génie mécanique

Mémoire présenté en vue de l'obtention du diplôme de *Maîtrise en sciences appliquées*
Génie aérospatial

Août 2022

POLYTECHNIQUE MONTRÉAL

affiliée à l'Université de Montréal

Ce mémoire intitulé :

Design and Validation of a Hydrogen Peroxide Vapour Decontamination System

présenté par **Mathieu CHARTRAY-PRONOVOST**

en vue de l'obtention du diplôme de *Maîtrise en sciences appliquées*

a été dûment accepté par le jury d'examen constitué de :

Cédric BÉGUIN, président

Étienne ROBERT, membre et directeur de recherche

Émilie BÉDARD, membre

DEDICATION

To my family and friends for supporting me during the whole project.

To my colleagues for their invaluable help and support.

To my supervisor for his great wisdom and kindness.

...

ACKNOWLEDGEMENTS

I would like to thank my research supervisor, professor Étienne Robert, for welcoming me within his research group LEMUR. His counseling was of great help all throughout the project, and his kindness is responsible for the pleasant atmosphere and camaraderie that permeates LEMUR. Even with his tremendous workload, he always finds time for his students, and his words are always pertinent.

I would also like to thank professor Benoît Barbeau and his research group for their help with the decontamination tests, lending me equipment and precious advice. A critical result would not have been possible without them.

I recognize the great work done by friend and colleague Gabriel Dubé in the inception of the project, helping kickstart it with a good foundation. His quality assistance helped me find my bearings in a field largely foreign to me.

This work would not have been possible without the bountiful advice given by my dear friends and colleagues in the LEMUR group, from which I have learned much. Their kindness and open-mindedness made me feel part of the group instantly.

RÉSUMÉ

La pandémie de la COVID-19 a eu de nombreux effets sur la société, dans plusieurs domaines. La pénurie d'Équipements de Protection Individuelle (EPI) causée par l'augmentation soudaine de la demande a été catastrophique, et de nombreux membres du personnel de la santé se sont retrouvés avec des EPI inadéquats, voire inexistantes. Les masques de protection N95 étaient une denrée particulièrement rare, car de nombreux consommateurs n'appartenant pas au secteur des soins de santé ont également essayé de les emmagasiner. La décontamination des équipements à usage unique tels que les masques N95 est devenue une mesure de crise qui pouvait au moins fournir des équipements stériles, même s'ils étaient usagés.

Les systèmes de décontamination des EPI se présentent sous de nombreuses formes, avec différents cas d'utilisation et caractéristiques. Les systèmes au peroxyde d'hydrogène vaporisé offrent une bonne couverture, une bonne pénétration des couches et une bonne efficacité de désinfection, ce qui les rend viables pour la décontamination des masques N95. Des systèmes commerciaux utilisant cette technologie existent, mais ils sont volumineux, dispendieux et rares en dehors des grands centres de soins.

Afin de fournir des capacités de décontamination dans les environnements à faibles ressources tels que les cliniques mobiles, les petits hôpitaux et les pays en voie de développement, un système au peroxyde d'hydrogène vaporisé a été construit en utilisant des composants commerciaux, dans une optique à libre accès (open source). La méthode utilisée pour atteindre une concentration élevée de peroxyde d'hydrogène (H_2O_2) gazeux est appelée "flash vaporization". Son utilisation a nécessité la conception d'une boucle pour retirer la vapeur d'eau de l'atmosphère et régénérer l' H_2O_2 gazeux en continu. Ces composants ont été placés dans une enceinte étanche aux gaz contenant les capteurs nécessaires au contrôle et au suivi du cycle. Il a été utilisé avec succès pour désinfecter des masques N95, prouvant la validité de la méthode et ouvrant la possibilité d'un déploiement rapide en cas de crises futures, pour un coût abordable.

Des expériences ont révélé les paramètres de contrôle critiques pour obtenir une efficacité maximale du système au-delà du seuil de décontamination. La température de vaporisation, la concentration initiale de la solution de peroxyde d'hydrogène et le taux de désintégration du gaz se sont avérés très importants pour atteindre les résultats souhaités. Dans l'ensemble, le système conçu démontre qu'un système au peroxyde d'hydrogène vaporisé peu coûteux peut être construit à partir de composants commerciaux et désinfecter efficacement les EPI. La conception a été mise en libre accès (open-source) et est disponible pour les utilisateurs

qui souhaitent construire le système tel quel, ou le modifier selon leurs besoins.

ABSTRACT

The effects of the COVID-19 pandemic were immense on many spheres of society, and are still felt today. Personal Protective Equipment (PPE) shortages caused by the sudden large increase in its demand were dire, and many healthcare personnel found themselves with inadequate PPE, or none at all. N95 Filtering Facepiece Respirators (FFRs) were a particularly scarce commodity, as many non-healthcare consumers also tried to stockpile them. Decontamination of single-use equipment such as N95 masks became a crisis measure that promised to at least provide sterile equipment, even if in used state.

Decontamination systems for PPE come in many forms, with different use cases and defining characteristics. Vaporized hydrogen peroxide (VHP) systems offer good coverage, layer penetration and disinfection efficiency, making it viable for N95 mask decontamination. Commercial systems using this technology exist, but are large, thus expensive and rare outside of major healthcare centers.

To provide decontamination capabilities to low-resource settings such as mobile clinics, small hospitals and developing countries, an open-source VHP design was built using commercial off-the-shelf (COTS) components. The method used to reach a high concentration of gaseous hydrogen peroxide (H_2O_2) is called flash vaporization. Using it required the use of a loop design to remove water vapour from the atmosphere and continuously regenerate gaseous H_2O_2 . These components were placed in a gastight enclosure containing sensors necessary for cycle control and monitoring. It was successfully used to disinfect N95 masks, proving the method valid and opening the possibility to rapid deployment in case of future crises, for an affordable cost.

Experiments revealed the critical control parameters to achieve maximum system efficiency above the decontamination threshold. Vaporization temperature, initial hydrogen peroxide solution concentration and the decay rate of gaseous H_2O_2 were found to be very important to reach desired results. Overall, the system designed demonstrates that an inexpensive VHP system can be built from COTS components and efficiently disinfect PPE. The design has been open-sourced and is available for users who wish to build it as is, or modify it to their needs.

TABLE OF CONTENTS

DEDICATION	iii
ACKNOWLEDGEMENTS	iv
RÉSUMÉ	v
ABSTRACT	vii
TABLE OF CONTENTS	viii
LIST OF TABLES	x
LIST OF FIGURES	xi
LIST OF SYMBOLS AND ACRONYMS	xii
LIST OF APPENDICES	xiii
CHAPTER 1 INTRODUCTION	1
1.1 Pandemic Context	2
1.2 Supply Issues due to the Pandemic	5
1.3 Problem statement	6
1.4 Personal Protective Equipment Decontamination	7
1.5 Research Objectives	8
1.6 Thesis Outline	9
CHAPTER 2 LITERATURE REVIEW	10
2.1 Personal Protective Equipment (PPE)	10
2.2 Decontamination Systems	12
2.3 Hydrogen Peroxide Physical Chemistry	16
2.3.1 Hydrogen Peroxide Characteristics	17
2.3.2 Flash Vaporization	23
2.3.3 H_2O_2 detection methods	23
2.4 Droplet impacts	24
2.5 Critical literature assessment	25

CHAPTER 3	METHODOLOGY	27
3.1	Theoretical limits	27
3.2	Preliminary test bed	28
3.3	Material and geometry tests	30
3.4	Closed loop tests	34
3.5	System design	36
3.6	Results	37
CHAPTER 4	ARTICLE 1: CONSTRUCTION AND VALIDATION OF AN AFFORD- ABLE HYDROGEN PEROXIDE VAPOR DECONTAMINATION SYSTEM . . .	38
4.1	Introduction	38
4.2	Methodology	40
4.2.1	Production of H_2O_2 decontaminating atmosphere	40
4.2.2	H_2O_2 vapour generator	43
4.3	Results	50
4.3.1	Cycle concentration and saturation	50
4.3.2	Pathogen reduction	52
4.3.3	Evaporation efficiency	52
4.4	Discussion	53
4.4.1	Cycle Reliability	54
4.4.2	System efficiency	55
4.5	Conclusion	56
CHAPTER 5	GENERAL DISCUSSION	57
CHAPTER 6	CONCLUSION AND RECOMMENDATION	58
6.1	Summary of Works	58
6.2	Limitations	59
6.3	Future Research	60
REFERENCES	62
APPENDICES	70

LIST OF TABLES

Table 1.1	Data of 10 countries with the most cases of COVID-19	2
Table 2.1	Respirator class description	11
Table 2.2	Disinfection systems overview	12
Table 2.3	Equilibrium concentrations of hydrogen peroxide vapour over liquid hydrogen peroxide at $t = 25\text{ }^{\circ}\text{C}$	17
Table 2.4	Properties of hydrogen peroxide and water	18
Table 3.1	Effect of initial relative humidity on the concentration of H_2O_2 con- densate	28
Table 3.2	Properties of tested metals	31
Table 3.3	Evaporation times of H_2O_2 droplets	34
Table 3.4	List of components used in final system	36
Table 4.1	Equilibrium concentrations of H_2O_2 vapour over liquid H_2O_2 at $t = 25$ $^{\circ}\text{C}$	42

LIST OF FIGURES

Figure 1.1	COVID-19 test rates for given countries (per million population) . . .	3
Figure 1.2	Global daily new cases	4
Figure 1.3	Global daily new cases per million people	4
Figure 2.1	Example of a VHP decontamination cycle	14
Figure 2.2	Phase diagram of $H_2O-H_2O_2$ system	22
Figure 3.1	First experimental test bed	29
Figure 3.2	Copper block and aluminum plate	32
Figure 3.3	Droplet test experimental setup and schematic	33
Figure 3.4	System schematic	35
Figure 3.5	System components in decontamination area	35
Figure 4.1	Closed loop system schematic	44
Figure 4.2	Flash vaporizer assembly	46
Figure 4.3	Powered desiccant column (silicagel not shown)	47
Figure 4.4	Typical concentration rates for injection and drying phases	49
Figure 4.5	Peak concentration vs. injection flow rate	50
Figure 4.6	Concentration and relative saturation during test	51
Figure 4.7	Evaporation efficiency at constant temperature	53
Figure 4.8	Evaporation efficiency at constant concentration	54
Figure 4.9	Comparison of droplet behaviour below and above the Leidenfrost point	56
Figure A.1	Peak concentration vs. injection flow rate	71
Figure A.2	Concentration vs. time at 0.1 ml/min	72
Figure A.3	Concentration vs. time at 0.5 ml/min	72
Figure A.4	Relative saturation vs. time at 0.5 ml/min	72
Figure A.5	Concentration vs. time with no added plates	73
Figure A.6	Concentration vs. time with 6 added plates	73
Figure A.7	Concentration vs. time with 30 added plates	74

LIST OF SYMBOLS AND ACRONYMS

PPE	Personal Protection Equipment
WHO	World Health Organization
CDC	Centers for Disease Control and Prevention
FDA	Food and Drug Administration
H_2O_2	Hydrogen Peroxide
VHP	Vaporized Hydrogen Peroxide
aHP	Aerosolized Hydrogen Peroxide
FFR	Filtering Facepiece Respirators

LIST OF APPENDICES

Appendix A Additional test data 71

CHAPTER 1 INTRODUCTION

Humanity has gone through many pandemics since the dawn of civilization. A pandemic is defined as "an epidemic occurring worldwide, or over a very wide area, crossing international boundaries and usually affecting a large number of people" [1]. These events often affect humans on a global scale and lead to many hardships, ranging from social distancing and non-lethal symptoms to complete societal collapse and widespread death [2]. They are caused by infectious diseases, usually by either bacterial or viral pathogens. In the last 40 years alone, many pandemics have plagued the world, such as those caused by the Human Immunodeficiency Virus (HIV), the Severe Acute Respiratory Syndrome Coronavirus (SARS-CoV and SARS-CoV2), the Influenza A virus subtype H1N1, the Middle East Respiratory Syndrome Coronavirus (MERS-CoV) and the Ebola virus [3]. Some of these pandemics, such as those caused by the HIV and Influenza viruses, are still ongoing, indicating great difficulty in solving these global problems and effectively getting rid of the underlying pathogens.

There are many factors that can increase the risk of a pandemic, or worsen its effects on society. Most of these factors are the results of modern human societies, such as climate change, overpopulation and antibiotic resistance [4–6]. For example, the United Nation's Intergovernmental Panel on Climate Change (IPCC) has concluded with a high degree of confidence that climate change would result in a greater frequency of infectious disease epidemics, which are defined as more localized than pandemics [4]. Overpopulation is also a likely factor, as explained by Spornovasilis *et. Al* [5].

Proper decontamination of infected surfaces and equipment can potentially greatly reduce a pandemic's impact on healthcare systems, or even prevent it. Another increasingly important factor that can cause pandemics is antibiotic resistance, and proper surface decontamination can contribute to solving it. Rapid evolution of antibiotic-resistant bacterial pathogens in hospitals create so-called superbugs, which may then spread to less developed regions and pose a significant threat to global health [6]. Providing a cheap, effective and decentralized method of decontamination would contribute to reducing a pandemic's effects on society, especially in less resourceful contexts. Development of such a method is the focus of this thesis.

1.1 Pandemic Context

The most recent pandemic, which is still ongoing as of 2022, is driven by the Severe Acute Respiratory Syndrome Coronavirus (SARS-CoV2), which causes the COVID-19 disease. The first known cases were identified in Wuhan, the capital of the Hubei province in China. It is believed to be a zoonosis, meaning it was originally found in animals, and the virus made a zoonotic leap to humans. In this case, analysts believe it originated from a public wet market [7].

True to the pandemic definition, this virus has spread throughout the globe and affected billions of people, whether it be by direct infection or by changing their lifestyle through the measures implemented to lessen the spread of the disease [8]. Partly because of the delayed onset of symptoms, high rate of transmission and possibility of re-infection, this virus has quickly spread from its first known case in Wuhan to the rest of the world. Many scientists now believe this virus will become endemic, meaning it will continue to circulate in certain populations for many generations [9]. Table 1.1 shows a typical cumulative snapshot of the epidemiological situation in some countries as of March 2022, approximately 2 years after the initial lockdowns in North America.

Table 1.1 Data of 10 countries with the most cases of COVID-19 [10]

Country	Cases	Deaths	Cases/1M pop	Deaths/1M pop
World	450,748,690	6,039,565	57,827	774.8
USA	81,016,779	987,741	242,374	2,955
India	42,975,883	515,386	30,636	367
Brazil	29,144,964	652,936	135,497	3,036
France	23,164,872	139,618	353,575	2,131
UK	19,373,884	162,482	282,892	2,373
Russia	17,140,069	358,246	117,366	2,453
Germany	16,291,067	125,515	193,403	1,490
Turkey	14,458,881	95,954	168,394	1,118
Italy	13,159,342	156,357	218,186	2,592
Spain	11,181,510	100,992	238,997	2,159

We can see from the data in table 1.1 that a high percentage of the population has been directly affected, with often more than 10% of the inhabitants of some countries with confirmed infections, reaching more than 35% for France. Of those cases, approximately 1% lead to a fatal outcome. This means that from 0.1% to 0.3% of the total population of severely affected countries has died from the disease since it first made its appearance. Most of the countries in this top ten have a good track record in regards to population testing, as seen

from the data in figure 1.1. We can therefore generalize this data to countries where the disease has become well-established, if not endemic, even when testing data is lacking.

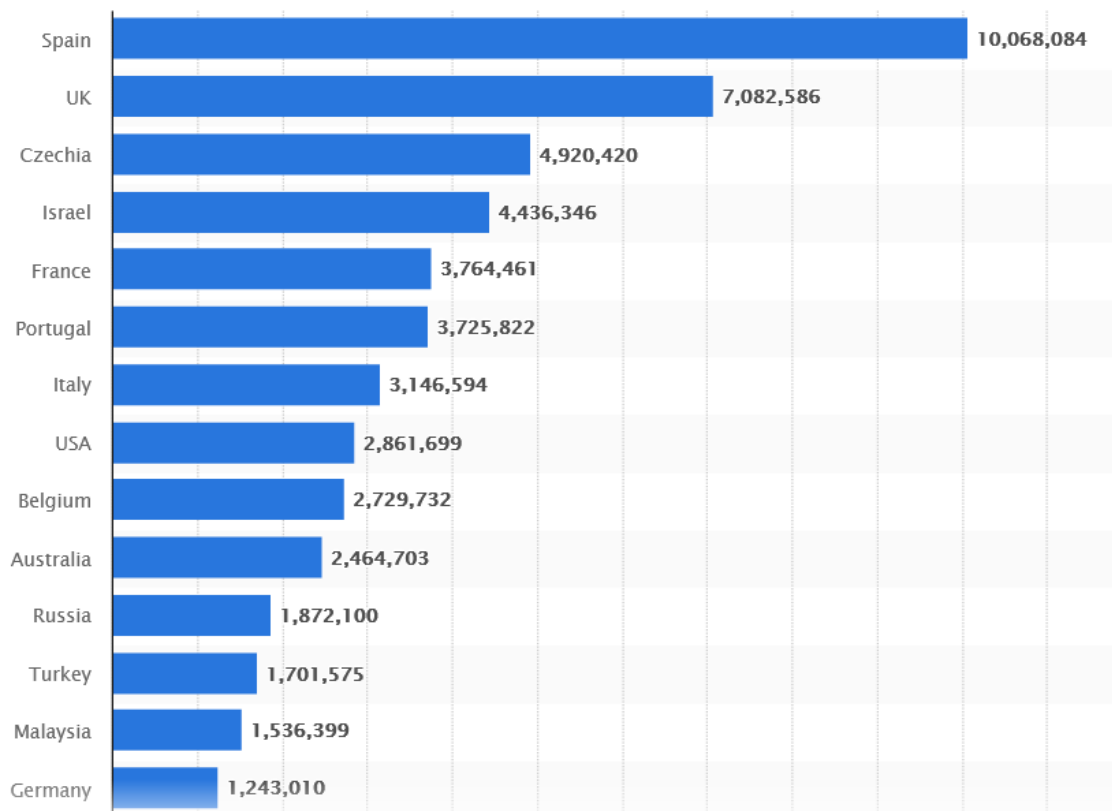


Figure 1.1 COVID-19 test rates for given countries (per million population) [11]

It is however recognized that COVID-19 cases are under-reported [12–14]. It is estimated that in some countries such as the USA, only 1 in 4 case were reported [12]. This is likely true on a global case, with less developed countries reporting even fewer cases, due to unavailability of testing resources. The results presented above should therefore be considered as conservative minimums in terms of infection numbers and death.

We can see the global reach of the pandemic in figures 1.2 and 1.3. When new variants of the virus with increased transmissibility appear unexpectedly in some countries, this can lead to a spike in new cases, colloquially called a wave. Since most countries' new cases tend to follow the same trend, with the global average following suit, we can therefore infer that the virus spreads very quickly on a global scale.

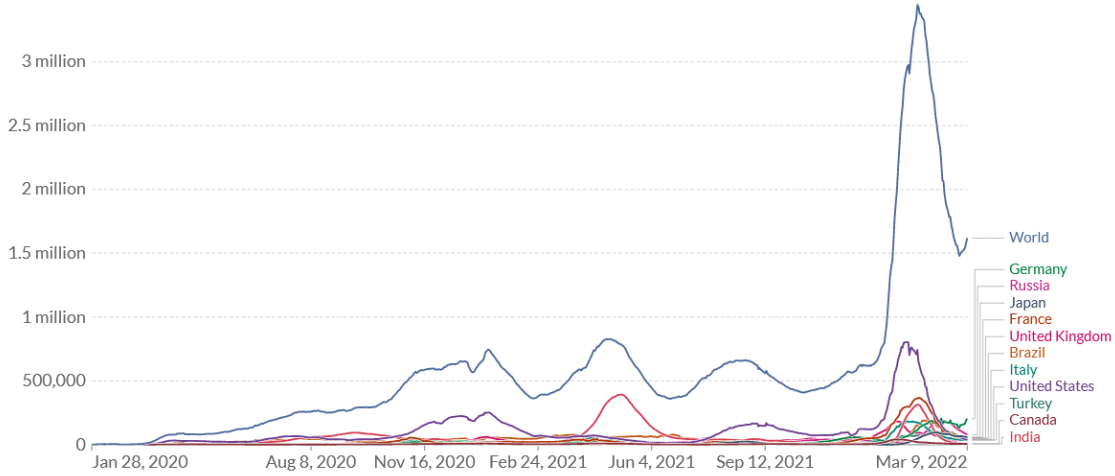
Many factors can lead to variations in new cases, severity of symptoms and likelihood of death. Among these, personal risk factors such as pre-existing medical conditions, physical activity

Daily new confirmed COVID-19 cases

7-day rolling average. Due to limited testing, the number of confirmed cases is lower than the true number of infections.



LINEAR LOG



Source: Johns Hopkins University CSSE COVID-19 Data

CC BY

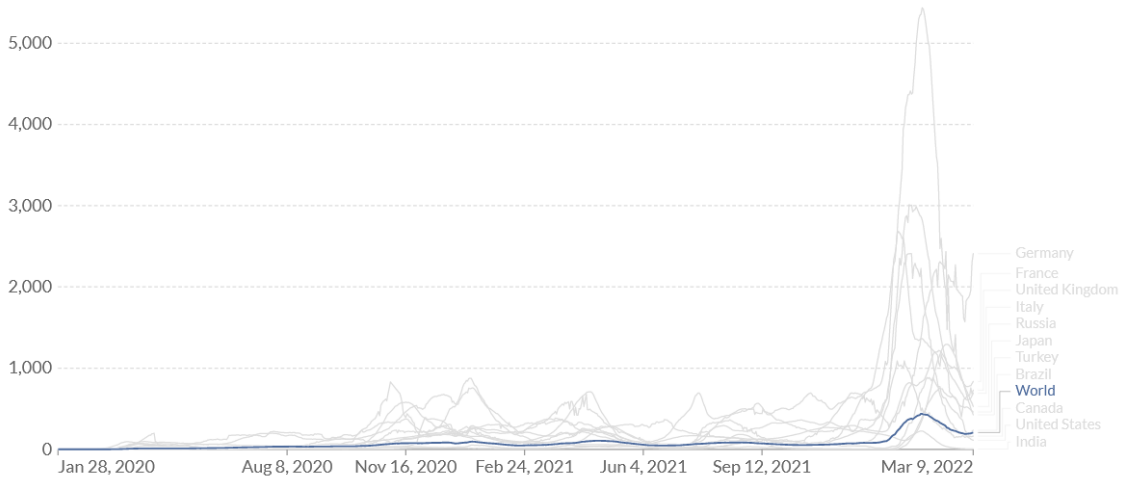
Figure 1.2 Global daily new cases [15]

Daily new confirmed COVID-19 cases per million people

7-day rolling average. Due to limited testing, the number of confirmed cases is lower than the true number of infections.



LINEAR LOG



Source: Johns Hopkins University CSSE COVID-19 Data

CC BY

Figure 1.3 Global daily new cases per million people [15]

level and habits (smoking) play an important role in disease severity [16]. Additionally, many more global factors contribute to variations in transmission and fatality, such as population density, climate and prevention measures in place [17]. Vaccines also protect against severe symptoms, with effectiveness depending on the infecting variant, the type of vaccine, the number of doses and time since last dose administration [18,19].

1.2 Supply Issues due to the Pandemic

The pandemic has taken a heavy toll on the global supply chain. Most economic sectors have been impacted, some more heavily than others, with projections foreseeing many years to complete recovery [20,21]. There are many contributing factors to this problem, some of which were already present before the pandemic and were exacerbated by pandemic-related events [22,23]. A supply chain critical to society, and very important for the resolution of this pandemic, is that linked to healthcare and social assistance. More precisely, the Personal Protection Equipment (PPE)¹ industry was heavily affected by the pandemic, with supply unable to keep up with the increased demand, right from the start. Because of the highly contagious aspect of the virus, PPE became recommended throughout society early on. SARS-CoV-2 Being a virus that mainly infects the respiratory system, masks were especially effective protection tools to limit spread, and demand rose accordingly, with some countries passing regional laws requiring their use in certain conditions, such as public indoor settings [24]. In healthcare, highly effective equipment were recommended such as N95 masks, replacing traditional surgical masks in most situations. This led to a shortage of PPE in general, with N95 masks becoming particularly rare. With the lack of vaccines and difficulty respecting sanitary measures, this put healthcare personnel at an elevated risk of contracting the disease [25,26]. This dangerous situation with healthcare personnel contracting the disease being removed from the workforce results in additional strain on the system, which could increase hospitalization rates and mortality. The PPE shortage is still felt as the time of writing this thesis, though with decreased importance [27]. Nonetheless, new variants and dwindling vaccine protection could result in a resurgence of cases, and an accompanying rise in PPE demand.

¹Detailed information on PPE is available in section 2.1

1.3 Problem statement

The supply issues causing a lack of PPE exacerbates many aspects of the pandemic, especially in healthcare. According to the Centers for Disease Control and Prevention (CDC), PPE is the least efficient way of controlling occupational hazards such as a virus, with the physical removal of the hazard being the most efficient [28]. It is nevertheless essential, even if a last resort. In crisis situations especially, it is often impossible to avoid contact with the hazard, and adequate PPE is therefore critical. There are a number of ways to lessen the impact of supply shortages, including reducing PPE usage with patient cohorting or telemedicine [29]. However, not all methods are equally feasible or effective. Reusing PPE can technically be implemented everywhere. However, to ensure proper protection with reused equipment, it cannot simply be kept from one job shift to another. It must be decontaminated to remove all traces of pathogens.

The issue addressed in this thesis is the difficulty of reusing PPE in a safe and accessible manner. PPE reuse is not typically done when adequate supply is available [30]. It is considered unnecessary or non-viable in normal, non-pandemic contexts. This is due in part to the additional logistics of processing PPE for decontamination, and the required change in workflow for healthcare professionals. Moreover, there is added difficulty in disinfecting porous materials, such as those that make up most filtering components. Some methods will greatly decrease filtration efficiency, such as chlorine or alcohol-based techniques [31]. Electrical properties such as the static charge in the microfibers must be maintained for effective filtration of fine aerosols.

3M, one of the largest PPE manufacturers in the world, recommends discarding equipment such as N95 respirators after use, while specifically recommending they do not be decontaminated for reuse [32]. During crisis situations, when shortages are dire, emergency authorizations can be delivered for the decontamination of PPE, by organizations such as the American CDC or the Food and Drug Administration (FDA).

Therefore, under most circumstances following health authorities and manufacturer guidelines, PPE are discarded after each use. This leads to a lack of capabilities for decontamination when acute need for it arises. Suitable decontamination tools are only available in a few select healthcare centers, and users in more rural or otherwise low-resource settings are dependent on a constant supply of new PPE [33, 34]. Commercial specialized decontamination devices exist, but are expensive and not readily available. Such tools therefore cannot be depended upon on a reactive basis at the moment, and new decontamination approaches must be made available on a preventive basis.

1.4 Personal Protective Equipment Decontamination

There are many available methods of decontaminating PPE, each with their own advantages and inconveniences. Most popular ones ensure a high reduction of pathogens, high reliability and the possibility to treat diverse types and models of PPE. Some room disinfection devices can also be repurposed as equipment decontamination systems, provided adequate facilities [33]. The most effective and well-researched methods include aerosolised Hydrogen Peroxide (aHP), Vaporized Hydrogen Peroxide (VHP), Ultraviolet germicidal irradiation (UVGI), Hydrogen Peroxide Gas Plasma (HPGP), Microwave Generated Steam and Ethylene Oxide (EtO) [35–37]. Of these, aHP, VHP and UVGI were the subject of renewed research in the early phase of the COVID-19 pandemic, presenting the best potential for respirator decontamination.

Vaporized Hydrogen Peroxide (VHP) systems use gaseous H_2O_2 as a decontaminating agent. Using a H_2O_2 vapour generator in an enclosure, they create a sterilizing environment as their primary method of eliminating pathogens. Use cases depend on workload and device, and are defined by parameters such as cycle processing time (including aeration time), environment temperature and H_2O_2 concentration. They can be used to decontaminate whole rooms, and are a common method for sterilizing hospital wards and operating rooms [37]. During the pandemic, this technology has been widely used to decontaminate Filtering Facepiece Respirators (FFR). VHP systems feature some of the best wide-spectrum decontamination capabilities, with high reduction of resistant hospital pathogens. Additionally, N95 respirators have been extensively tested with VHP systems, and they show no or little signs of wear after processing, being able to withstand sometimes as many as 30 cycles before some parts of the masks are deemed unusable [30, 38–40].

Aerosolized Hydrogen Peroxide (aHP) systems, as their name suggests, use aerosols consisting mainly of droplets of aqueous H_2O_2 solutions as primary decontaminating agents. Since there is no phase change from the liquid solution to the aerosol, compared to VHP's evaporation, more complex liquid solutions can be used, containing additional biocides, or components that can help the aerosol coat surfaces such as surfactants. For the former, silver is often used in undisclosed amounts, as these machines often use proprietary disinfectant solutions. They are easier to operate than VHP systems, but are typically less effective in getting rid of pathogens. They are more affected by "dead zones" in enclosures, and have less penetration power than VHP, resulting in difficulty decontaminating porous filter equipment. Their main advantage is less stringent infrastructure requirements for their use, since VHP requires very good ventilation capabilities [41, 42].

Ultraviolet germicidal irradiation (UVGI) systems use short-wavelength Ultraviolet (UV-C) radiation as their main decontamination method. The wavelength used depends on the targeted pathogen, and light-generating device. For example, mercury-based lamps emit light peaks at 254 nm, while pulsed-xenon lamps have their peak around 230 nm [43]. Since different pathogens have different germicidal efficiency curves, the peak wavelength is a very important parameter.

The main advantage of UVGI systems is their non-invasive nature. Compared to most other systems, they use no chemical agent, and are therefore among the safest for both the operators and the staff. Some systems even have motion sensors that deactivate them if movement is detected, for example if a door is opened. They also do not leave potentially toxic residues, if used with compatible and approved equipment (that won't degrade under UV-C radiation). Their main disadvantage is their vulnerability to 'dead zones', when line of sight is broken with the radiation's origin. This is also a problem to decontaminate porous filtration material and fabric. They are less effective than VHP systems at eliminating pathogens [44,45]. Such UVGI systems have been successfully built using local and standard components, as done by Schnell *et al.* [46].

1.5 Research Objectives

The general objective of this work is to design a decontamination system capable of processing filtering facepiece respirators such as N95 masks, complete with associated protocols. It was rapidly determined that, given the crisis situation caused by the COVID-19 pandemic, the system would need to be compact, safe, easy to use, and made of affordable components. This would provide a new decentralized method that can be easily deployed to low resource settings that do not have access to commercial solutions, such as most institutions outside major healthcare centers. The VHP method was prioritized, considering expertise in related domains such as aerosol generation and mitigation, high temperature combustion using hydrogen peroxide, and gas composition analysis. The VHP system designed needs to meet all safety requirements of competent authorities such as OSHA, NIOSH and Health Canada, while also achieving decontamination performance comparable to commercial solutions.

Creating an atmosphere of gaseous H_2O_2 is not easy, due to the challenges associated with the vaporization of hydrogen peroxide. Notably, it is a thermally unstable compound that will naturally decompose, with the reaction rate increasing with temperature [47]. This reaction is also catalyzed by many materials [48]. These factors make it difficult to obtain a high concentration of gaseous H_2O_2 and maintain it for a sufficient amount of time to achieve decontamination.

The target of this system being low resource settings, it needs to be inexpensive. However, being a healthcare product, the price decrease must not be at the cost of reliability or safety. It must have performance comparable to commercial alternatives, being able to efficiently decontaminate PPE in a safe way, and for a high number of cycles. Decreasing the cost will mean a scaling down of commercial systems, introducing fluid mechanics problems that will need to be resolved in order to obtain a successful system.

Taking into account that this is mostly a solution to a resource problem making PPE scarce, the system design needs to optimize resources used, such as hydrogen peroxide, drying agent and electricity.

The final product must provide a practical way to decontaminate equipment, since additional logistic strain in an already complex healthcare system would defeat the product's purpose of reducing strain on said healthcare environment. It should be a self-contained device, meaning it will contain all necessary components for its use, except power and reagents. It will be a mostly "plug-and-play" system, able to process batches of PPE, with the batch size depending on the enclosure size and the type of PPE. Finally, it must be safe for operators, with the possibility for simple "set-and-forget" use.

Uses beyond PPE decontamination are limited, but nonetheless very interesting and would require little to no modification of the designed system. The main alternative is room decontamination, since VHP systems can theoretically be used to decontaminate any enclosure. Due to the open-source and modular aspect of this work, it should be possible to scale up certain operating parameters or components, rendering it possible to decontaminate larger enclosures such as entire rooms. Procedures would of course need to be adapted to these situations to ensure safety.

1.6 Thesis Outline

This thesis will first explore the literature related to PPE and decontamination systems. A very in-depth look at hydrogen peroxide and its properties will follow, being the primary source of complexity in this work. The next chapter will detail the design of the decontamination system built for this thesis. Chapter 4 contains the main results, including an assessment of the decontamination performance, and system resource efficiency. It will also contain discussion on all those subjects. Finally the conclusion is comprised mainly of a summary, the limitations of the presented solution, and the future research that would need to be done in order to obtain a product certified by appropriate regulatory agencies.

CHAPTER 2 LITERATURE REVIEW

A review of the literature is presented here for three main subjects, namely Personal Protective Equipment (PPE), decontamination systems, and hydrogen peroxide physical chemistry. Adequate knowledge of these subjects is necessary to properly design an equipment decontamination system using gaseous hydrogen peroxide. A review of PPE was needed in order to properly understand the properties of equipment to be decontaminated, more specifically N95 respirators. These masks follow a standard that must be taken into account when determining the operating parameters of the final system, to ensure their longevity. Following this, a review of decontamination systems is done to compare various technologies and assess the most optimal method of decontamination in our context. Vaporized hydrogen peroxide was chosen for the present work, and is further explored. Since hydrogen peroxide is an unstable component and vaporizing it to obtain a sustained gaseous concentration comes with certain difficulties, an in-depth review of its characteristics and interactions is presented. A review of droplet impacts was also done, since the technique used for conversion to gas of a liquid solution uses a drop-by-drop impact method, and knowledge on the impact dynamics is important.

2.1 Personal Protective Equipment (PPE)

PPE comes in many forms, from hazardous materials (hazmat) suits and hard hats to surgical masks and work boots. In a general sense, it refers to any garment or supplementary equipment that serves to protect the user from hazards, be they chemical, radiological, physical, electrical, mechanical, or any other workplace hazards [49]. The focus of this thesis is mainly N95 filtering facepiece respirators, but the systems and protocols developed herein likely apply to a wider range of equipment, though specific equipment must be approved individually for decontamination through tests, to ensure compatibility of the method with the concerned equipment.

The U.S. National Institute for Occupational Safety and Health (NIOSH) is responsible for the classification of filtering respirators used in most of North America. The U.S. Code for Federal Regulations (CFR) maintains the certification and approval processes [50]. N95 respirators are therefore classified under section 42 CFR 84.170(a)(3)(iii). This is summarized in table 2.1. This section governs non-powered air-purifying particulate respirators, and efficiency means the proportion of airborne particles that are filtered by the respirator, by particle count. In this classification, the letter N represents a respirator that is **N**ot resistant

Table 2.1 Respirator class description

Class	Minimum filter efficiency (%)
N95, R95, P95	95
N99, R99, P99	99
N100, R100, P100	99.97

to oil, while R is **R**esistant to oil and P is oil-**P**roof. A respirator classified as N95 is therefore any mask that is 95% efficient at filtering airborne particles, and that is not resistant to oil.

N95 respirators protect the respiratory airways, namely the mouth and nose. They must therefore provide a good seal on the user's face to ensure all particles pass through the respirator's filter and not around the mask. The seal quality is quantified by the fit factor metric. Without a sufficiently high fit factor, masks are not approved under the N95 class. N95 masks typically have two elastic polymer straps to secure themselves over a user's mouth and nose, with the addition of a metal clip to pinch the bridge of the nose.

The filters used in N95 respirators are typically made of electrocharged filtration layers of polymers such as polypropylene or polystyrene [51]. They consist of nano- and microfibers forming a tightly wound net that traps particles while still allowing air through. Pore diameter must be carefully studied to find the correct value to trap large particles (diameter greater than 1 μm), small particles (diameter less than 0.1 μm) and intermediate particles in-between.

N95 masks were previously decontaminated using guidelines from various manufacturers and public health authorities [52,53]. Companies that develop decontamination systems, such as Battelle or Steris, perform their own tests to certify usage of varied types, or classes, of PPE with their systems. This ensures proper usage of the device, within specific guidelines. These systems are then reviewed and approved by health and safety authorities, such as OSHA and Health Canada, to permit their use in relevant countries. As such, the research presented here is based on systems which have passed Health Canada regulations, and that use the same method that we wish to implement, namely H_2O_2 vapor decontamination. This was done to accelerate the development process, and simplify the subsequent required approvals by health and safety authorities.

Certain parameters, depending on the system, must typically be met to ensure proper decontamination (ex: H_2O_2 concentration, UV strength). Some of the environments created by decontamination systems can be quite hostile to materials. For example, since hydrogen peroxide reacts strongly with many materials, a high concentration of it may negatively affect the equipment by degrading it [54,55]. This must be taken into consideration when designing

decontamination systems, but also when selecting PPE. Not all N95 masks are equal, only their minimum filtering efficiency are prescribed along with other parameters regulated by the N95 classification of the CFR. Some respirators are more durable and resistant to decontamination, being able to withstand upwards of 30 cycles, while some suffer critical degradation after only a few cycles, depending again on the method used for decontamination [31, 56].

2.2 Decontamination Systems

A comparative overview of disinfection methods is available in table 2.2, adapted from a review made by Otter *et al.* [37] under permission. Characteristics of an 'ideal' disinfection systems were determined by the author, and four different decontamination methods were reviewed in light of these characteristics. In table 2.2, a crossmark (✗) indicates that the system does not meet the criteria, while a checkmark (✓) indicates that it does. If both are present (✗/✓), it is not clear if the criteria is met.

Table 2.2 Disinfection systems overview [37]

Ideal system characteristic	Aerosolized hydrogen peroxide (aHP)	H ₂ O ₂ vapour	UVC	Pulsed xenon UV (PX-UV)
Short cycle time (<1h)	✗	✗	✗/✓	✓
High level of microbial efficacy (6-log sporicidal reduction)	✗/✓	✓	✗	✗
Pathogens not culturable from surfaces after the cycle	✗	✓	✗	✗
Easy to operate	✓	✗	✓	✓
Fully automated operation	✓	✓	✗/✓	✗
Immediate room entry available	✗	✗	✓	✓
No requirement of room sealing	✗	✗	✓	✓
Homogeneous distribution	✗	✓	✗	✗
US EPA registered	✗	✓	✗	✗
UK Rapid Review Panel recommendation	✗/✓	✗/✓	✗	✗
Evidence of clinical impact	✗	✓	✗	✗

This review concerns No-Touch automated room Disinfection (NTD) systems, but these technologies can also function as equipment decontamination with little to no modification to their principles of operation. A down-scaling of the components is the main difference between the room and equipment versions. This is mostly due to the fact that these systems are made to disinfect rooms that meet certain criteria, such as good control of airflow, a sufficient seal around doors or windows, and the absence of certain reactive materials. These restrictions are in place to prevent the disinfectant, be it hydrogen peroxide, UVC radiation or any other, from leaking out and causing harm. A smaller equipment decontamination enclosure is therefore comparable to these rooms, even providing better control on the restricted parameters, for potentially better decontamination.

From the data available in table 2.2, we can observe that various methods yield quite dif-

ferent criteria fulfillment. In some cases, there is a clear advantage to a specific method in relation a criteria, even with such a binary assessment. This can be seen in the "homogeneous distribution" characteristic, where only the H_2O_2 vapour systems meet the criteria, or adversely in the "easy to operate" characteristic, where it is the only method to fail. In a general view, systems based on hydrogen peroxide vapour fulfill the most criteria, with six out of eleven being respected, with a seventh being only partially met. However, it is important to note that this does not mean it is necessarily the best system, as different use cases will place increased priority on certain characteristics. For example, the short cycle times of UV systems might be desirable in some industries, when the lower level of pathogen reduction is not a deal-breaker. Moreover, the requirement for a sealed room in hydrogen peroxide systems might make the use of this method impossible in some cases.

Vaporized Hydrogen Peroxide

Of the methods used in healthcare, vaporized hydrogen peroxide is typically the decontaminating method with the widest range of virucidal, fungicidal and biocidal properties. Hydrogen peroxide has been used as a general purpose disinfectant for many years, and even over-the-counter very dilute solutions of 3% are quite effective at getting rid of pathogens. It has been the subject of many studies, and its biocidal properties are well understood [57]. This is why it is a staple in the healthcare sector. Its vaporized form is also a popular way of decontaminating rooms, provided adequate room conditions [58].

The basic principle behind the method is the transformation of an aqueous solution of hydrogen peroxide to gaseous form, which is then injected in an enclosure. This is done until a sufficiently high concentration to disinfect is reached, and this minimum concentration is maintained for a set amount of time to allow the peroxide to spread and inactivate pathogens [59]. After this disinfection phase, the concentration is lowered to safe levels for enclosure opening, which is less than 1 ppm for gaseous hydrogen peroxide [60].

Various manufacturers and systems have different operating parameters not only to fill different market needs, but also because the process of decontaminating with gaseous hydrogen peroxide is not yet fully understood, especially related to condensation, as explained in section 2.3.1 on Aqueous Solutions and Raoult's law. One of the most important parameter is the concentration of gaseous hydrogen peroxide during the disinfection phase. Related to this are the operating conditions such as relative saturation, humidity, temperature and pressure, with a discussion of these parameters available in section 2.3.1 as well. These parameters are interdependent, and some might be the main design focus that will determine the others. These are important to consider when looking at what needs to be decontaminated. For

example, a system which uses a wet gas (high relative saturation) will create condensation within the enclosure. This might cause some material compatibility issues, since gaseous H_2O_2 will condense at a higher concentration than its initial liquid form [61], as discussed in section 2.3.1. Finally, the length of the different phases and overall cycle are also important specifications, since customers typically want the shortest cycle possible.

Figure 2.1 shows an example of a typical VHP decontamination cycle, based upon our own work and VHP patents [59].

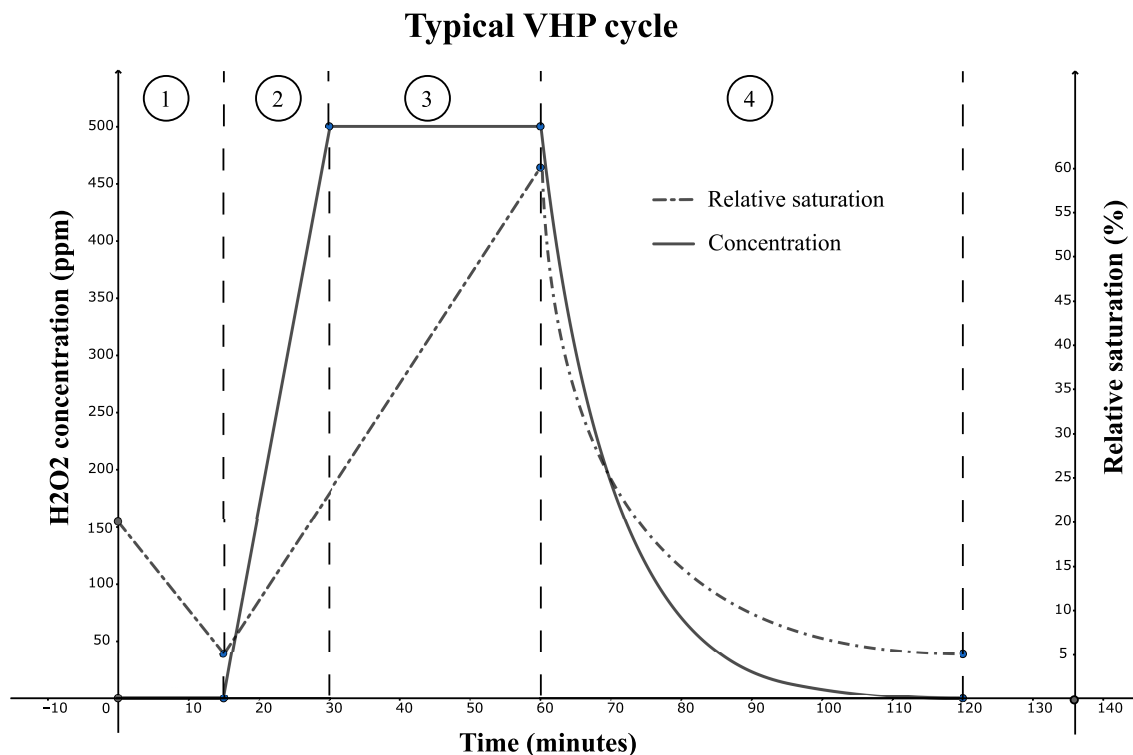


Figure 2.1 Example of a VHP decontamination cycle

This is an example of a VHP system which operates at ambient pressure, near-ambient temperature and low relative humidity. The first phase (1) is the atmosphere preparation, which serves to lower the relative humidity and adjust the temperature. This is usually done quickly, lasting from 10 to 15 minutes. Once the desired values are attained, the atmosphere conditioning (2) is started, during which the gaseous H_2O_2 concentration will rapidly increase until the desired value is obtained, usually under 20 minutes. Following this is the sterilizing phase (3), where the operating parameters will be kept at their nominal values for a set amount of time. This phase can last anywhere from 20 minutes to many hours, depending on the size of the enclosure, maximum concentration and decontamination load. Variations

in the relative saturation parameter between manufacturers occur based on the technique used for drying the gas, if the gas is dried in the first place. If the drying system is efficient enough, relative saturation might remain constant for this phase. If not, it might increase steadily as in figure 2.1, as the water vapour slowly accumulates in the atmosphere. The final step is the aeration phase (4), which consists in removing the H_2O_2 from the enclosure and equipment. This is typically the longest phase, since the Permissible Exposure Limit (PEL) for H_2O_2 is quite low at 1 ppm, and security factors are typically in place in the form of a time buffer to ensure this value is reached everywhere in the enclosure, and that all residual H_2O_2 that could be present on the equipment is decomposed or otherwise aerated. This can last anywhere from 90 minutes to 24 hours.

Another critical characteristic of gaseous hydrogen peroxide is its excellent penetrating power, which is important to ensure proper decontamination of masks made of fibrous materials, and layered filters. Compared to methods based on aerosols, a gas will have an easier time reaching the deeper layers of filters, whereas an aerosol might only get deposited on the upper surface. Moreover, it can also fill an enclosure or room completely, being mostly independent of device placement within that enclosure. There are no blind spots, compared to UV decontamination. This leads to a greater coverage of the equipment, and ensures all parts of it are decontaminated.

Many studies and reports have been published detailing the capabilities and limitations of vaporized hydrogen peroxide. A report prepared by the nonprofit science and technology company Battelle published in 2016 detailed the importance of decontamination in the event of a pandemic, and gives important data on the decontamination of N95 respirators using VHP technology (a Bioquell Clarus C HPV decontamination system) [40]. They found that the filtration efficiency does not degrade even after 50 cycles of decontamination, but the limitation to number of reuses is rather the elastic straps, which degrade after 20-30 cycles. There has been an evident increase in VHP publications following the onset of the COVID-19 pandemic, due to the technology's potential in helping the PPE supply crisis. A recent paper by Yen *et al.* finds results similar to the Battelle report, with a different system [62]. Vaporized hydrogen peroxide is one of the favoured approaches for N95 respirator decontamination. A study comparing it to aerosol based hydrogen peroxide found VHP was safer to operate, slightly faster and achieved a greater level of biological inactivation than the aHP system [41]. The review by Otter *et al.* described previously found similar results, with a variation in cycles from 1.5 hours to 8 hours, depending on the system used [37]. This discrepancy is explained by the authors with the difference in operating relative saturation and subsequent condensation within the systems. All VHP systems tested attained a log-6 reduction in contaminants, which is considered as satisfactory in such decontamination

protocols.

Other forms of VHP decontamination have also been investigated, such as a dual-sterilant system which uses vaporized hydrogen peroxide in conjunction with ozone [63]. This led to increased lethality and a more complete decomposition of residuals, which both contribute to making the cycle usable on a wider selection of equipment.

The main parameter on which this work is based is the concentration of gaseous hydrogen peroxide during the main decontamination phase. Based on the available literature, a good decontamination target should be to create an atmosphere of at least 500 ppm of gaseous hydrogen peroxide, maintained for at least 20 minutes. This is according to the standard operating procedure of Duke University's Regional Biocontainment Laboratories [64]. This environment is created by a Bioquell Clarus C system, and is the benchmark for the procedures described here. Other systems use higher concentrations, sometimes as high as 5700 ppm, but the lower concentration of the proven Clarus C system can be achieved more easily with commercially available H_2O_2 [65, 66].

2.3 Hydrogen Peroxide Physical Chemistry

Hydrogen peroxide is obviously the active ingredient in VHP decontamination, along with water and air. Understanding its physical and chemical properties is therefore crucial, especially since it is a very reactive substance. Simply evaporating a solution of hydrogen peroxide and water is not sufficient to obtain a high concentration of gaseous H_2O_2 , as will be explained in the following sections.

As described by Hultman *et al.*, 1 mg/L of hydrogen peroxide vapour can be as effective as 400 mg/L of aqueous solution for decontamination of bacterial spores [61]. The vapour clearly acts in a more efficient manner. They also describe the difference between simple evaporation and a technique called flash vaporization. The latter is a way to obtain a higher gaseous concentration, and will be explained in more details in section 2.3.2. Evaporation of aqueous H_2O_2 solutions does not typically lead to a high gaseous concentration because of the difference in vapour pressure between water and hydrogen peroxide. Because H_2O_2 has a lower vapor pressure than H_2O , the latter is concentrated in the gas phase by the evaporation process. Since high concentrations of liquid hydrogen peroxide are dangerous, both as an explosive hazard and a very powerful oxidizer, the solutions used in decontamination systems are usually composed of 30% to 50% H_2O_2 , more often on the lower end of this spectrum. At equilibrium, these solutions will yield much lower concentration in the vapour headspace than the liquid, as seen in table 2.3. Additional regulations on concentrations higher than

30% also make it highly impractical to work with such solutions, and methods such as flash vaporization must be used to obtain the desired gaseous concentrations [67]. Even if regulations weren't in place, dangerously high liquid concentrations would need to be used to achieve a high gaseous concentration, as shown in table 2.3, and would render the system hazardous.

Table 2.3 Equilibrium concentrations of hydrogen peroxide vapour over liquid hydrogen peroxide at $t = 25\text{ }^\circ\text{C}$ [61]

Liquid (% w/v)	Vapour (% w/v)
32.1	1.87
55.7	8.0
73.9	24.1
77.8	35
88.3	56.4

Condensation is an important parameter of VHP systems, since it can affect not only decontamination efficiency, but cycle time and even system longevity. Watling *et al.* [68] explain that there are two schools of thought related to condensation in such systems. Some manufacturers operate a dry gas without condensation, in order to better control the process. Others operate at saturation in order to induce condensation. Some believe condensation is mostly unavoidable, and it is even the primary cause of decontamination. Watling's paper describes into great detail the theoretical equations that govern condensation in VHP systems. The four typical phases in the decontamination process are individually studied, with accompanying equations and graphs. The initial H_2O_2 concentrations that will lead to condensation are presented at various starting relative humidity, for different types of systems.

2.3.1 Hydrogen Peroxide Characteristics

Hydrogen peroxide is a molecule that is quite similar to water, with the only difference being an additional oxygen atom. Nevertheless, this difference makes the substance behave quite differently in many ways, even though it retains some similarities. While they are both transparent liquids at standard temperature and pressure (STP), hydrogen peroxide has a sharp odour, compared to water's essentially odourless nature. It is the simplest of peroxides, and the most common. Important properties of both pure hydrogen peroxide and water are available in table 2.4.

From this data, we can see that the liquid form of hydrogen peroxide is quite similar to water, with viscosity and surface tension of comparable values. The thermochemical properties are also similar, with the heat of vaporization, and heat capacity being less than 20% apart in

Table 2.4 Properties of hydrogen peroxide and water [69–73]

Name	Hydrogen peroxide	Water
Chemical formula	H_2O_2	H_2O
Molar mass (g/mol)	34.015	18.015
Melting point (°C)	-0.43	0.00
Boiling point (°C)	150.20	100.00
Density (g/cm ³) at 25°C	1.44	0.99701
Vapour pressure (torr) at 25 °C	1.97	23.75
Heat of vaporization (kJ/mol)	51.60 (at 25 °C)	40.65 (at 100 °C)
Heat capacity (J/mol·K) at 25°C	89.328	75.385
Viscosity (cP)	1.249	0.890
Surface tension (dynes/cm)	80.4	71.97

magnitude. A notable difference between the two substances is the increased boiling point of hydrogen peroxide, at 150.2 °C compared to water's 100 °C. The biggest change in property is the vapour pressure, with H_2O_2 having a value an order of magnitude below that of water at room temperature, 1.97 torr compared to 23.75 torr. This difference is an important part of why it can be difficult to obtain a gaseous atmosphere of hydrogen peroxide, as will be explained in this chapter.

While water is an excellent solvent, hydrogen peroxide is a very potent oxidizer and reducer, and has the tendency to react strongly with many materials, rather than form solutions as water. This property makes hydrogen peroxide difficult to work with, and material compatibility must be tested to ensure no degradation of components or hazardous behaviour. For example, the medical equipment company Steris Corporation tests all potential materials that would be used in their VHP systems [55]. It is expected all medical equipment companies do this, as hydrogen peroxide can cause oxidation of metals that do not traditionally react with water or air, such as aluminum or stainless steel [54].

Precautions must be taken when storing hydrogen peroxide, as it will thermally decompose over time. It is considered thermally unstable, and is often mixed with stabilizers to prevent or slow this process down. It can spontaneously combust when mixed with organic materials, and can explosively decompose at high concentrations. Its thermal decomposition products are oxygen (O_2) and water (H_2O).

Care must also be taken when handling high concentration hydrogen peroxide solutions, since there are many harmful effects to its exposure. Any contact with the liquid, whether it be ingestion, eye contact or simply skin exposure will all cause negative effects, with higher concentrations leading to worse outcomes. This is due to its powerful oxidizing nature, which

will make it react strongly with the organic matter omnipresent in humans. Its vapour is also toxic, and breathing it must be avoided. Adequate protection must be used when handling the liquid, especially gloves, glasses and skin protection. When the vapour is involved, a respirator must be donned to prevent the vapour reaching the lungs and causing harm.

Thermal Decomposition

Hydrogen peroxide is a thermally unstable substance, and will decompose into oxygen (O_2) and water (H_2O) naturally, by the general equation 2.1. A lot of work has been done by the National Research Council (NRC) of Canada on the subject of hydrogen peroxide in both its liquid and vapour form. Author Paul Giguère was at the forefront of many of these papers, such as an article detailing the kinetics of the decomposition hydrogen peroxide vapour [74].



This is a self-sustaining reaction, as its standard enthalpy of reaction (ΔH^0) is -2884.5 kJ/kg, meaning it is exothermic. If left unchecked, a non-stabilized solution will eventually completely decompose. Most commercial solutions contain small amounts of stabilizers for this reason.

The article by Giguère finds that the reaction is of the first order and that the reaction rate is governed by equation 2.2 for the tested pressures and temperatures, which are respectively 10 mmHG and 400 °C. This Arrhenius equation is helpful in finding the rate of decomposition of equation 2.1, and will help in optimizing the system's operating parameters to either minimize or maximize decomposition, depending on which cycle phase is being studied.

$$k = 10^{13} e^{-\frac{48000}{RT}} \text{ sec}^{-1} \quad (2.2)$$

where k is the rate constant, T is the temperature in kelvins, and R is the universal gas constant.

A number of other studies related to hydrogen peroxide vapour has been published by the NRC in the Canadian Journal of Research by the same laboratory. A two-part study on the thermal decomposition of this vapour, by Baker *et al.* [47] and Giguère [75] respectively, has been very important to this study, since much practical knowledge can be gained from it, in addition to theoretical values and equations.

In the first part by Baker and Ouellet [47], a broader approach is taken to find the general kinetics of the reaction. This was done at lower temperatures than Giguère's kinetics study

mentioned earlier, from 70 °C to 200 °C with low pressures of 1 to 2 cmHg. Their aim was to correlate the reaction rate with temperature in various containers, to determine how different surface geometries affect the reaction. It was already known that the reaction rate increased with temperature, and this was expected. An interesting result they found is that even with the same material and cleaning process (chromic acid washed Pyrex glass), changing the surface-volume ratio affects the reaction rate, with no definite quantitative relation. The geometry itself therefore plays an important role as well. Another important part of the article is the study of carrier gas on the reaction. The H_2O_2 decomposition was done in air, O_2 and CO_2 . No significant difference was found between the rate constants of these experiments. This means that the reaction is unaffected by these neutral gases, and consequently, according to the authors, that the reaction is not a chain mechanism but rather controlled by geometric effects and diffusion to the walls of the flasks. This result pertaining to gases is especially useful for our work, since it means that adding a carrier gas to the system would not affect the thermal decomposition, and this design is therefore possible.

The second part of the study, by Giguère [75], focuses on material types and surface treatment. As expected, they find that both parameters affect reaction rates, sometimes by large factors. For example, fusing glass reduces its activity by a factor of 20. Over time and regular use, this effect disappears and the rate goes back to the same as non-fused glass. Washing the flasks with hot chromic acid, salts(saturated trisodium phosphate solution) or aqueous hydrofluoric acid also seemed to increase activity. With testing of various glass, such as pyrex and quartz (both fused and non-fused), they found that different glass types give different reaction rates, and that fusing likely decreases this constant due to the smoothing of the surface. Moreover, tin and aluminum containers were tested. These supposedly inert metals gave different reaction rates, with tin having higher values. They were not however much different than their glass counterparts.

Catalytic Decomposition

Hydrogen peroxide can act as both an oxidizer and a reducer, and can therefore react with many types of materials. As such, it can itself be catalyzed easily, increasing its rate of decomposition by contact with adequate substances. This catalysis must be accounted for and controlled adequately to achieve a sufficient concentration of hydrogen peroxide. Pedziwiatr *et al.* [48] explain the kinetics of the catalysis of hydrogen peroxide with popular catalysts. They explain that H_2O_2 decomposes according to a disproportionation reaction, in which the products contain oxygen atoms of different oxidization states. According to them, and their references, this decomposition is affected by many factors, such as: catalyst exposition,

temperature, pressure, concentration of solution, type, activity and area of active catalytic surface of the catalyst, exposure to direct sunlight and presence of inhibitors. Many types of catalysts may be used to increase decomposition rate, namely heterogeneous (silver, gold, iron), homogeneous (iodide, iron ions) and enzymes (catalase). In their study, the catalysts tested were silver, manganese compounds, potassium dichromate, iron oxides and TiO₂-UV. With the abundance of iron and its alloys in clinical studies, it is a good review on the effect this metal might have on reaction rate. As Makjan *et al.* [76] demonstrated, even stainless steel will corrode under exposition to H₂O₂. More factors and catalysts were also investigated by Yazici *et al.* [77], such as the effects of initial H₂O₂ concentration, temperature and pH. Other solids were also tested.

It is unambiguous according to the literature that surfaces exposed to hydrogen peroxide must be of a controlled and specific material, that has no catalytic interactions with the peroxide. This will ensure an adequate gaseous hydrogen peroxide concentration, and also contribute to system longevity, reliability and safety. Material choice will become a very important parameter in the design of the decontamination system.

Aqueous Solutions and Raoult's law

Due to the difficulty of obtaining high concentration hydrogen peroxide, the hazards associated with its handling and its tendency to decompose, H₂O₂ is only available commercially as relatively weak aqueous solutions (3%-30% w/v). To obtain a high concentration of hydrogen peroxide vapour, this is not ideal. As shown in table 2.4, hydrogen peroxide has a much lower vapor pressure than water. This means that in a typical atmosphere at STP, water will preferentially evaporate and occupy most of the vapour headspace. Increasing the liquid concentration of the peroxide solution will increase the gaseous concentration, but comes with associated risks, since a very high concentration must be used to obtain an adequate result, as shown in table 2.3. Another important facet of these solutions is the fact that the remaining liquid will be of higher concentration than the initial solution. This is again caused by the difference in vapor pressure, with hydrogen peroxide being concentrated to potentially dangerous levels by this preferential evaporation.

A good way of visualizing the equilibrium of aqueous H₂O₂ solutions is with phase diagrams. As explained by Hultman *et al.* [61], a 35% (by weight) concentration of H₂O₂ will yield a 2% gaseous concentration, and a 77.8% concentration in the condensate. The phase diagram of the H₂O₂ – H₂O system is shown in figure 2.2, from an article by Jildeh *et al.* [78], used with permission. The two curves are the phase transition curves, and give the temperature necessary for a phase change at a given mole fraction. As the fraction of H₂O₂ increases, so

does the temperature needed for it to transition.

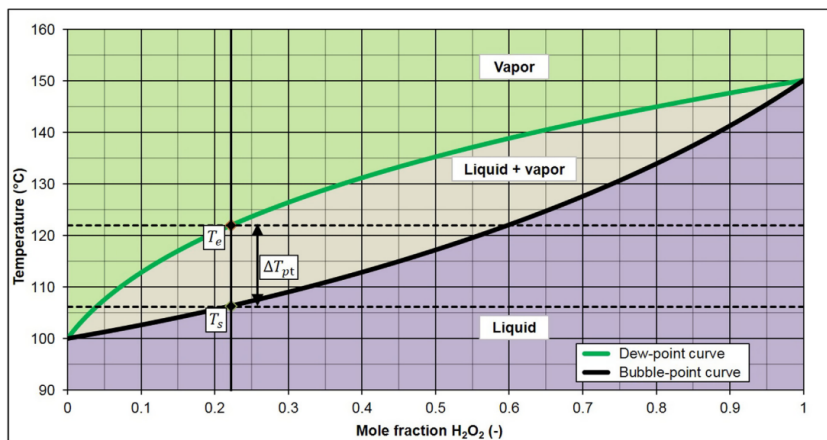


Fig. 2. Calculated binary isobaric VLE (T vs. x) diagram of a H_2O_2/H_2O system at atmospheric pressure of 1013.25 hPa. The black vertical line at 22.19 mol% represents the heating/cooling line for an aqueous 35% w/w H_2O_2 solution.

Figure 2.2 Phase diagram of $H_2O-H_2O_2$ system

The main equation that governs the liquid-gas equilibrium of liquid mixtures is Raoult's law:

$$p = p_A^*x_A + p_B^*x_B + \dots + p_i^*x_i \quad (2.3)$$

where p is the vapor pressure of the solution, p_i^* the i^{th} component's vapor pressure, and x_i is its mole fraction in the solution. Because of hydrogen bonding, Raoult's law has to be adapted to the $H_2O-H_2O_2$ system with activity coefficients [68]:

$$p = \gamma_W p_W^* x_W + \gamma_H p_H^* x_H \quad (2.4)$$

where γ is the activity coefficient, and subscripts W and H refer to water and hydrogen peroxide respectively.

We can see from equation 2.4 that at equilibrium, water will occupy most of the vapor headspace, since its high vapor pressure compared to hydrogen peroxide will make its partial pressure component ($\gamma_W p_W^* x_W$) disproportionately high. Since its vapor pressure is approximately 10 times higher than H_2O_2 , we would need to greatly increase the mole fraction of H_2O_2 to obtain even a 50/50 distribution in the gas atmosphere. As previously explained, the hazards associated with this render it highly impractical.

Spiegelman and Alvarez [79] describe a way of circumventing the limitations imposed by Raoult's law. In the context of gaseous hydrogen peroxide creation, they conceived a two-

stage vaporizing device that uses a carrier gas. This gives their system the ability to reach high concentration of gaseous H_2O_2 without the need for very high liquid concentrations. While their system is impressive, it is a degree of complexity above what the system designed in this thesis aims for, since it requires not only a carrier gas but two vaporizers. Nonetheless, the theory on Raoult's law in their paper was very useful for our work.

2.3.2 Flash Vaporization

A method used to achieve a high concentration of gaseous hydrogen peroxide is called "flash vaporization". The papers by Hultman [61] and Watling [68] both explain flash vaporization and its uses. They describe it as a direct application of a small amount of aqueous hydrogen peroxide solution to a heated plate whose temperature is above the boiling point of the mixture. Until saturation is reached in the gaseous atmosphere, this method ensures that the ratio of peroxide to water in the gas is the same as in the liquid solution. Compared to simple evaporation, this method has the possibility to yield much higher vapour concentrations. If the temperature of the plate is too high, adverse effects such as thermal decomposition or Leidenfrost may occur, lowering system efficiency.

Since saturation is inevitable in a closed system being continuously fed moist gas, systems using flash vaporization need a way to remove this moisture. Two types of hydrogen peroxide gas generators are used, as described by Watling. Both are variations of closed loops of hydrogen peroxide generation and atmosphere drying, permitting a constant stream of new H_2O_2 while removing the water vapour. In the first variation, a single loop is used to vaporize, dry and decompose the gas. In the second variation, two loops are used. The first contains the dryer and catalyst for the conditioning and aeration phases, while the second one contains only the flash vaporizer, as well as a way to heat up the gas. Both variations theoretically give the same results.

2.3.3 H_2O_2 detection methods

Specialized sensors are required to detect gaseous hydrogen peroxide. Such sensors have two primary uses. The first being as a safety device, in places where there might be hydrogen peroxide gas exposure. With the OSHA permissible exposure limit (PEL) being only 1 ppm, these sensors typically have a range of 0-10 ppm to 0-100 ppm, with precision of approximately 0.2 ppm. The second use is as a sensor for much higher concentrations, for monitoring decontamination or industrial processes. They can have ranges from 0 to upwards of 2000 ppm, with typical precision of 1 ppm. Since 500 ppm is the desired minimum concentration for typical VHP decontamination system, this second type of sensor is needed in such contexts.

Coles and Lehtinen [80] explain the advantage of combining this sensor with a humidity sensor. This gives complete real-time control of the process in a reliable way. Traditionally, VHP systems were controlled by parametric methods, with the critical control parameters being air/vapour flow rate and the peroxide solution delivery rate to the evaporator. Other parameters such as H_2O_2 vapour concentration were also recorded, but played no role in cycle control. The real-time data on both H_2O_2 vapour concentration and humidity provides means to further optimize the cycles, with potentially shorter cycles and better decontamination.

Lehtinen [81] has also written another paper on the subject, in which she details the critical parameters of VHP decontamination. These are temperature, relative humidity and relative saturation. The difference between relative humidity and relative saturation is that the former comprises only water's contribution to humidity, while the latter contains contributions of both water and hydrogen peroxide. Relative saturation is calculated as follows:

$$RS = \frac{p_w}{p_{ws}(H_2O + H_2O_2)} * 100\% \quad (2.5)$$

where p_w is the water vapour pressure and $p_{ws}(H_2O + H_2O_2)$ is the saturation water vapour pressure at a given H_2O_2 vapour concentration and gas temperature [82].

The distinction must be made because H_2O_2 has a similar molecular structure to water and affects humidity. The article explains the relation between these parameters, as well as temperature. Condensation will occur at 100% relative saturation, before reaching 100% relative humidity. It is therefore important to keep track of this parameter. She also briefly explains that humidity sensors used in VHP systems typically use a catalytic layer coupled with a normal humidity sensor, to distinguish between water and hydrogen peroxide.

2.4 Droplet impacts

Since the flash vaporization method described in section 2.3.2 consists of droplet impacts on a very hot surface, it is pertinent to peruse the literature on the subject of droplet impact dynamics. Quéré [83] has done a review on Leidenfrost dynamics which contains a useful section on droplet impacts. The main parameter that will affect droplet impacts is the Weber number (We), defined by the following equation:

$$We = \rho V^2 R / \gamma \quad (2.6)$$

where ρ is the fluid density, V is the velocity, R is the droplet diameter and γ is the surface tension. This number compares the kinetic energy of the liquid to its surface energy. Some

important observations in relation to the We number is that the elasticity of the impact (V'/V where V' is the velocity after impact) decreases with We , with a value close to 1 for $We < 1$, decreasing to near zero for high We . This means that droplets with high surface energy compared to their kinetic energy, such as small droplets with low impact velocity, will conserve more of this kinetic energy. In our case, since we wish to optimize heat transfer and surface contact, this can have a negative effect on system performance. Moreover, there is a We regime in which, if the surface temperature is high enough, droplets will eject many droplets, effectively forming an aerosol. This is also something that needs to be avoided for this project, since this aerosol will not convert to gas.

Droplet size and impact velocity will need to be carefully chosen to optimize the impact dynamics and obtain a high heat transfer. Experimental tests will be used to assess the dynamics of our system, since they are very system-specific, being affected by surface material, surface roughness, liquid density and viscosity and presence of external factors (such as air velocity).

2.5 Critical literature assessment

The main purpose of the decontamination system developed in this work is to process N95 masks, of all makes and models. The shell of these filtering facepiece respirators is usually made of porous polymers such as polyester, while the straps are usually made of thermoplastic elastomers. The filter itself must conserve its properties throughout the process in order to maintain its high filtration efficiency.

The chosen method for decontamination is vapourized hydrogen peroxide, for its potent decontamination power and its compatibility with porous materials. According to the literature, a gas concentration of 500 ppm is sufficient to obtain a log-6 reduction of pathogens. There is no clear agreement between manufacturers or researchers on the effects of condensation on the decontamination process itself. For the decontamination process considered here, a dry gas will be used since the processed material is porous, and condensation might negatively affect filtration efficiency. The temperature in the enclosure will be kept near ambient to preserve the respirators, and to prevent thermal decomposition of the peroxide.

Several tests and precautions will be necessary to obtain a working system, due to the properties of hydrogen peroxide. Common materials such as stainless steel, copper, most elastomers, nylon and many others are unsuitable for use in VHP systems, since they will act as catalysts for the hydrogen peroxide decomposition. This will not only lower the concentration in the gaseous atmosphere, but also degrade the material acting as a catalyst. All materials in the

enclosure must therefore be non-reactive with H_2O_2 , and without impurities.

The technique used to obtain a high concentration of gaseous H_2O_2 in the enclosure will be flash vaporization, to partially circumvent the limitations imposed by Raoult's law. Commercial systems successfully use flash vaporization, but their operating parameters are proprietary. This makes it difficult to reproduce a similar system, as no open-hardware VHP systems currently exist. Moreover, there is a lack of information available for small-scale VHP systems. Research must therefore be made to adapt the flash vaporization technique to the small-scale form factor.

The temperature of the heating element will need to be carefully chosen. In order to flash vaporize, the surface temperature must be much higher than the boiling point of the solution. However, an increase in temperature will lead to an increase in thermal decomposition of the H_2O_2 , as well as the onset of film boiling above the Leidenfrost temperature. Because of the small-scale aspect of the flash vaporizer, it is expected that droplets will be strongly affected by the Leidenfrost effect as they are more mobile [83]. Research is needed to identify the optimal flash evaporation temperature which will yield the highest gas concentration per volume of liquid injected.

CHAPTER 3 METHODOLOGY

This chapter serves as a complement of the methodology from the article available in chapter 4. This extension contains data and specific information that could not be included in the article, but that may be useful to reproduce the system, and that illustrate the path used in the design process.

Many steps were necessary before building the final system and achieving effective decontamination of N95 respirators. A review of the literature was needed to understand the theoretical gaseous concentration limits of hydrogen peroxide, as well as what could be expected in a commercial system. This depends on the main operating parameters of such systems, namely enclosure temperature, pressure and relative saturation. These parameters were therefore important to set beforehand, taking into account the desired gaseous concentration as well as our use case. Ambient temperature and atmospheric pressure were desirable in our case for many reasons. Low temperatures decrease the thermal decomposition of hydrogen peroxide and the degradation of N95 masks. Atmospheric pressure means no need for complex pressure control, which would greatly increase system cost. All that needs to be controlled then is the relative saturation, dependent upon the performance of the system's drying component. Material and geometry tests were done to assess the most efficient flash vaporizing method. This was necessary to obtain a high concentration of gaseous hydrogen peroxide while keeping a low relative saturation. If the system is inefficient at converting liquid hydrogen peroxide to gas, the atmosphere will saturate with water vapour, leading to low H_2O_2 concentration, as well as undesirable condensation.

Once this was completed, the performance of the H_2O_2 neutralization system was evaluated. Once sufficient drying performance was confirmed, the complete system was assembled, and decontamination tests began, with more tests done to characterize the evaporation efficiency achieved with the system.

3.1 Theoretical limits

According to table 2.3, an aqueous solution of 32.1 % w/v hydrogen peroxide should give a concentration of 1.87 % w/v H_2O_2 gas at equilibrium, or 18700 ppm. This is far above the concentrations seen in even the most efficient commercial systems, which can range from 500 ppm to 5700 ppm, as explained in section 2.2.

Watling *et. al* [68] as well as Lehtinen [81] both explain the codependency between the

gaseous H_2O_2 concentration, temperature, relative humidity and saturation [68, 81]. Table 3.1 shows some results from Watling’s theoretical calculations, which give the relation between initial relative humidity, temperature and concentration.

Table 3.1 Effect of initial relative humidity on the concentration of H_2O_2 condensate

Starting RH%	Concentration of Condensate %w/w		
	10°C	20°C	30°C
10	75.1	74.4	73.6
20	68.9	68.4	67.8
30	62.7	62.3	61.8
40	56.3	56.0	55.7
50	49.7	49.5	49.2

This table shows the concentration of the condensate. It can therefore be used to assess the concentration in the gas, based on phase diagrams and Raoult’s law. We can clearly see that a rise in initial relative humidity will lead to a decrease in concentration in the condensate and therefore in the gas. This factor contributes to the lower concentration achieved in real systems, with the other major factor being thermal or surface decomposition.

According to the literature, to achieve the highest concentration of gaseous H_2O_2 , relative humidity must be kept as low as possible. This is why a closed loop dryer system was designed, to continually remove water vapour from the atmosphere. Nevertheless, experimental values are always lower than theoretically possible, as factors such as evaporation efficiency and the decomposition of H_2O_2 greatly impact the gaseous H_2O_2 concentration in the enclosure. Work is needed to maximize efficiency and minimize decomposition.

3.2 Preliminary test bed

Once the desired operating parameters were chosen, namely a gaseous H_2O_2 concentration of 500ppm and no condensation, a preliminary test bed was built to confirm if they were achievable with our objective of using mostly commercial off-the-shelf (COTS) components. This step is necessary to assess the severity of H_2O_2 thermal or surface decomposition in a typical decontamination setting. It was also used to test different methods of generating H_2O_2 gas, as well as to explore the operation of our H_2O_2 gas sensors. This test bed is shown in figure 3.1. It consists of a cylindrical acrylic enclosure containing the H_2O_2 gas generator and the gas detector. This first gas generator is a long glass tube with heating wire tightly coiled around its length. The rate of injection of the liquid peroxide solution was controlled by a syringe pump. The energy fed to the wires was set by a 3 amp transformer with voltage

ranging from 0 to 240 volts, and the temperature was read by a type K thermocouple. The gas detector is a Vaisala HPP272 probe, and is a highly reliable commercial probe. It can give measurements of the hydrogen peroxide gas concentration, relative saturation and temperature. This hardware was kept for the final system, and additional information pertaining to it is available in section 3.5.

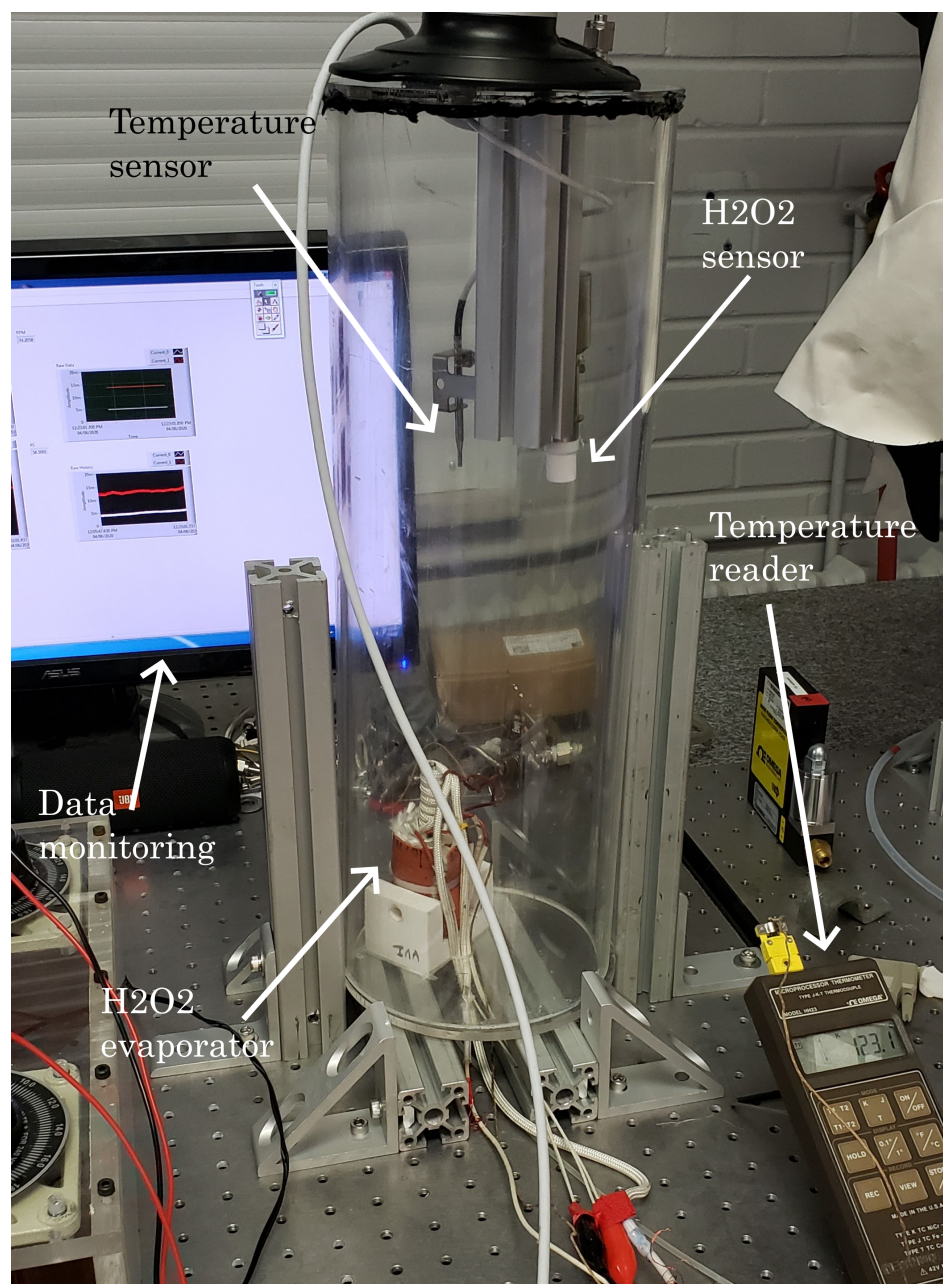


Figure 3.1 First experimental test bed

This test bed gave us important data on the limits of evaporation when working with hydrogen peroxide, as well as thermal decomposition insights. Since this system was a closed design with no regeneration loop, the atmosphere quickly saturated with a high proportion of water, preventing further increases in H_2O_2 concentration. When injection was stopped, we could also note the progressive decrease in H_2O_2 concentration, meaning thermal or surface mediated decomposition was underway.

3.3 Material and geometry tests

The literature review revealed that hydrogen peroxide is prone to thermal decomposition, and can be catalyzed by many materials. Experimental tests were carried out to determine which material was best to use for the heated surface of the flash vaporizer, where the liquid droplets are impacted. Ideally, this surface would have high thermal conductivity, high thermal capacity and low reactivity to hydrogen peroxide and water vapour.

The thermal properties are necessary to ensure that enough energy is supplied to the droplets in a rapid manner to enable flash vaporization rather than boiling. If thermal conductivity is not high enough, the surface where droplets vaporize might gradually cool down, and have colder temperature transients. Low thermal capacity might also result in a colder surface, since each droplet will take a proportionally larger fraction of the surface's thermal energy, leaving less for the next droplet if it is not replenished in time.

Low reactivity to hydrogen peroxide and water vapour is also essential to ensure system efficiency, reliability and longevity. If the surface is reactive to H_2O_2 , it will act as a decomposition catalyst and consequently lower evaporation efficiency. The H_2O_2 will eat away at the surface, leading to decreasing performance over time as oxides appear, when metals are present. It is important to note that the surface's high temperature will greatly accelerate catalysis reactions, and that materials non-reactive at ambient temperature might oxidize under operating conditions.

Four different metals were tested for use as the flash vaporizer's droplet impact surface: aluminum, copper, brass and stainless steel. The properties of these materials useful for this analysis are available in table 3.2.

Two useful physical quantities for this comparison are the volumetric heat capacity ($c_{p,v}$) and thermal effusivity (e), calculated from equations 3.1 and 3.2 respectively.

$$c_{p,v} = c_p * \rho \tag{3.1}$$

¹From Hydrogen Peroxide Material Compatibility Chart [54]

Table 3.2 Properties of tested metals [69, 84]

Material	Copper	304 Stainless steel	Yellow brass	6061 Aluminum
Thermal conductivity (κ) (W/mK)	401	15	120	155
Density (ρ) (kg/m^3)	8960	7900	8470	2730
Specific heat capacity (c_p) (kJ/kgK)	0.385	0.491	0.396	0.953
Volumetric heat capacity ($c_{p,v}$) ($\text{kJ}/\text{m}^3 \text{K}$)	3449.6	3878.9	3354.12	2601.69
Thermal effusivity (e) ($\text{J}/\text{m}^2\text{K}\sqrt{\text{s}}$)	37192.60	7627.81	20062.26	20081.38
Suitable for use with H_2O_2^1	No	Up to 48 °C	No	Yes

$$e = \sqrt{k * c_{p,v}} \quad (3.2)$$

The thermal effusivity is a measure of the thermal inertia, which is a value that must be as high as possible in a flash vaporizer surface, for reasons explained above. A high value usually means the material can store a lot of energy and easily distribute it among itself and to other components. Since the design of the plate is mostly fixed, a volume-specific property such as thermal effusivity is a good metric for comparison.

According to table 3.2, copper would then be the ideal material, since its excellent thermal conductivity (beaten only marginally by silver in metals), high density and decent specific heat capacity result in the highest thermal effusivity by far. However, it reacts strongly with hydrogen peroxide, acting as a strong catalyst. This makes it impossible to use as the droplet impact surface.

Brass has similar volumetric heat capacity to copper, but its lower thermal conductivity renders it a much less attractive contender. Moreover, it suffers the same high reactivity to H_2O_2 . It offers no advantage over any candidate and is therefore eliminated.

Stainless steel is characterized by a high density and specific heat capacity, giving it the highest volumetric heat capacity of the material candidates. However, its extremely low value of thermal conductivity results in the lowest value of thermal effusivity by far. Even though it can store the most energy per volume, it is very inefficient at conducting it out. This is why thermal effusivity must be analyzed and not simply volumetric heat capacity. Its decent passivity to H_2O_2 would have made it a possible candidate otherwise.

Aluminum has very good specific heat capacity, but its very low density gives it quite a low volumetric heat capacity. However, its high thermal conductivity results in thermal effusivity that is surpassed only by copper. Contrarily to the latter though, it is very chemically resistant to H_2O_2 . It is therefore the primary candidate for the droplet impact surface.

Following this review and some droplet tests, a combination of aluminum and copper was

found to be the best solution. To take advantage of copper's excellent thermal effusivity, the main heat source in which the cartridge heaters are inserted is a block of copper. To prevent oxidation from contact with H_2O_2 , a thin plate of aluminum is deposited on the copper block, and acts as the H_2O_2 droplet impact surface. The two are bonded by high-temperature high-conductivity thermal paste. This setup results in a high thermal inertia and very good chemical passivity. It is shown in figure 3.2.

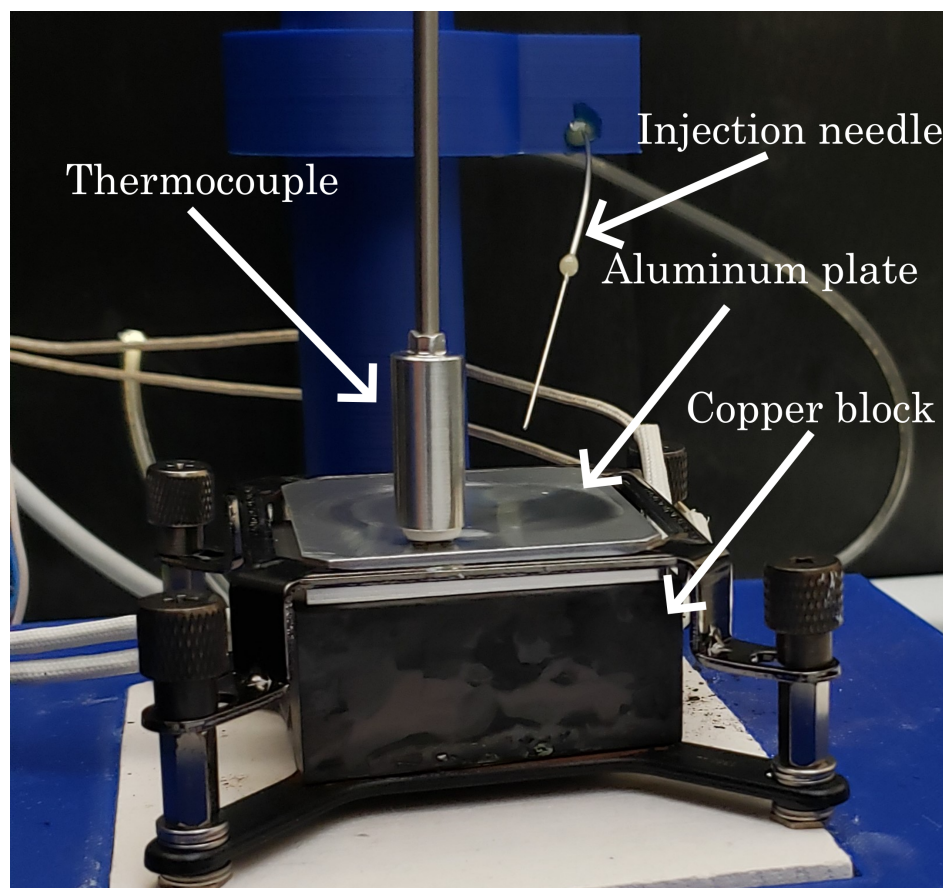


Figure 3.2 Copper block and aluminum plate

A plate of each material was made in order to test the validity of the above assertions. Droplet tests were devised to study the mechanics of flash vaporization on each material, as well as the effect of plate temperature, liquid solution concentration and droplet impact velocity. The droplet evaporation time was quantitatively measured, and the volume of liquid ejected away from the plate upon droplet impact was qualitatively studied. These analyses were done with the help of a Photron AX200 high-speed camera, as illustrated in figure 3.3. Sample results are available in figure 3.3. We were able to confirm that a copper

plate results in the quickest evaporation for a single droplet, while stainless steel results in the slowest evaporation. Moreover, lower concentrations of liquid H_2O_2 also resulted in faster vaporization. This was expected since the boiling point of the mixture increases with concentration in H_2O_2 . However, because of Raoult's law, this will not necessarily lead to higher gaseous concentrations.

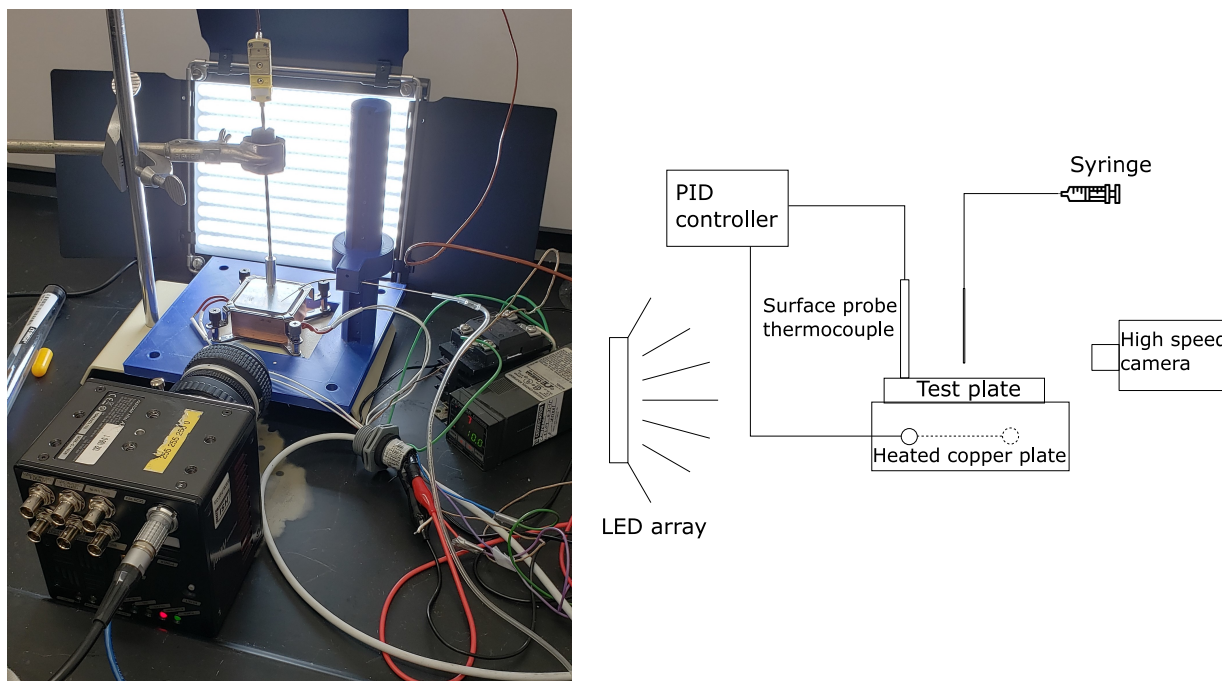


Figure 3.3 Droplet test experimental setup and schematic

The droplet impact velocity was varied by changing the height difference between the injection tube and the hot surface. Since droplets are injected slowly and one at a time, the change in velocity is easily measurable since no other parameters are affected. We found that a rise in droplet impact velocity had no significant effect on evaporation time, but only up to a certain point. With sufficient velocity, the droplet impacts fast enough to split and may be ejected from the hot surface altogether. Moreover, generally more micro-droplets are ejected as velocity increases. Keeping velocity as low as possible is therefore desirable in our case.

Two different geometries were tested with aluminum. The first is a flat plate, with the droplet impact surface polished with high-grit sandpaper. The second geometry contains a reamed hole where the droplets impact, acting as a recess for droplets that might bounce around because of the Leidenfrost effect. We found that the reamed plate resulted in a higher concentration of gaseous peroxide at higher temperatures where the Leidenfrost effect might be more pronounced, since the droplets cannot escape the reamed hole. However, this

Table 3.3 Evaporation times of H_2O_2 droplets

Plate material →	Aluminum		304 Stainless steel	Copper
Liquid H_2O_2 Concentration (%) →	10	30	30	30
Temperature ↓	Evaporation time (s)			
90	44.710	-	-	-
100	19.517	53.039	34.972	10.80567
110	3.801	31.417	20.811	6.611333
120	1.397	17.571	14.505	2.733
130	0.458	6.617	7.411	1.42
140	0.409	1.816	4.188	-
150	-	0.382	2.150	-
160	-	-	1.216	-
170	-	-	0.849	-
180	-	-	0.655	-
190	-	-	0.464	-
200	-	-	0.378	-
210	-	-	0.337	-

does not necessarily lead to the highest possible gaseous concentration, as droplets still take longer to vaporize than if temperature was kept below the Leidenfrost point. The polished geometry is therefore better, since better heat transfer allow it to evaporate droplets in a quicker manner, assuming no Leidenfrost.

3.4 Closed loop tests

Once the plate design was chosen, tests were made to validate our preliminary assertions and the dryer design. This is necessary, since there is much uncertainty with H_2O_2 systems in the literature, and many parameters affect the system. A near-perfect model of gaseous H_2O_2 concentration and relative saturation during a cycle is impossible to build without experiments that take into account these many parameters.

The system was built according to our own design shown in figure 3.4. The flash vaporizer is continuously fed the liquid H_2O_2 solution, while the drying and neutralizing loop removes water vapour from the atmosphere. Some components are external and pass on their data or reagent to the enclosure through gas-tight fittings. The components in the decontamination

area are shown in figure 3.5, and explained in the following section.

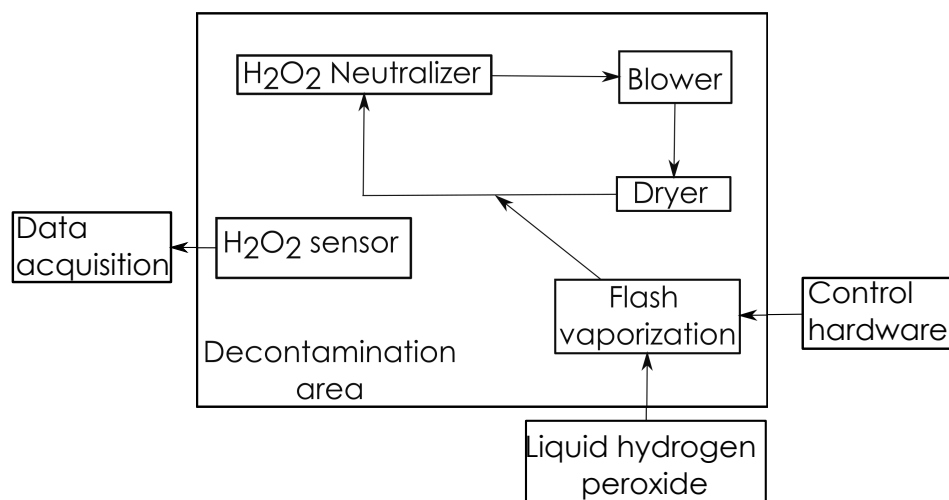


Figure 3.4 System schematic

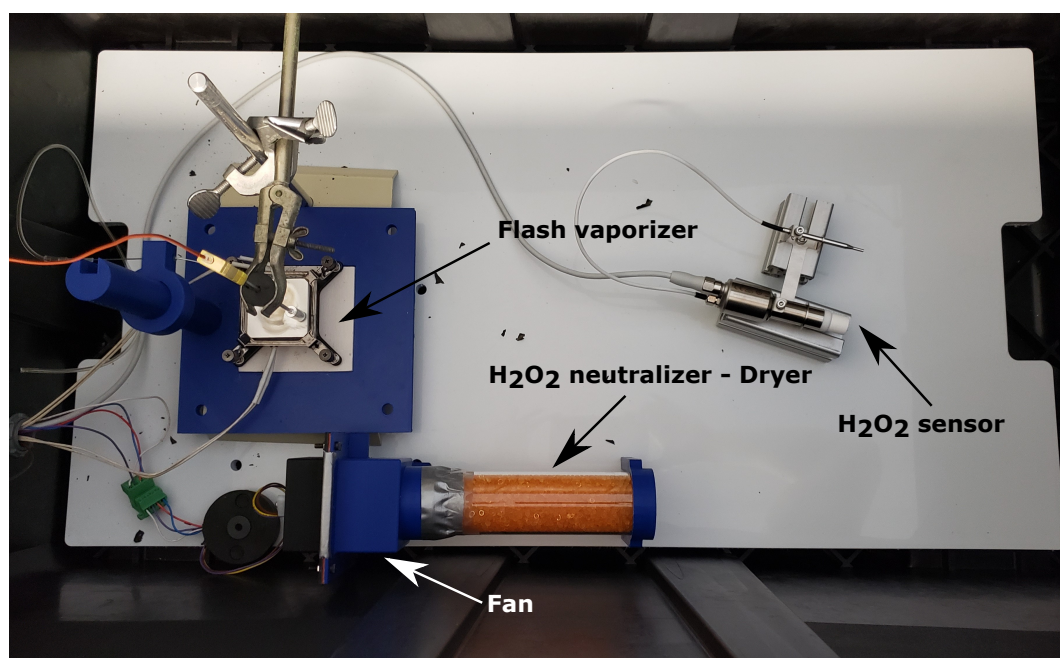


Figure 3.5 System components in decontamination area

Tests were made under different conditions to verify that the system's efficiency is conserved under various operating parameters and workloads. Tested parameters include H_2O_2 in-

jection rate, dryer power, desiccant state, surface area in the enclosure and flash vaporizer temperature. The optimal values for these parameters were found and used to obtain the results available in chapter 4. The data is available in appendix A.

3.5 System design

Table 3.4 lists the specific hardware used in the construction of the final system. An asterisk (*) means the component was custom-built using facilities available at our campus, and a dash (-) means the make and model of the component is unknown.

Table 3.4 List of components used in final system

Purpose	Component	Make	Model	Notes
Flash vaporizer	Copper block	*	*	2 holes for cartridge heaters
	Aluminum plate	*	*	
	Cartridge heaters (2x)	-	-	100W Incoloy sheath
	Thermal paste	Slice Engineering	Boron Nitride Paste	
	CPU cooler assembly	Beizuu	CPU Water Cooler Mounting Bracket Hardware Kit for Intel LGA 1150 1151 1155 1156 for Corsair Hydro H60 H80i H100i H110i GT	
Injection	Syringe pump	New Era Pump Systems	NE-4000	
	Watertight syringe	Monoject	20 ml Luer tip	Plastic
	Flexible tubing	-	-	Plastic
	Injection tube	-	-	Stainless steel; 0.85 mm outer dia.
	Injection tube holder	*	*	3D printed ABS
Blower	Centrifugal fan	ebm-papst	RV45-3/14S	
	Fan drive kit	ebm-papst	992.0640.004	
	Fan enclosure	*	*	3D printed ABS
Dryer/destroyer	Desiccant	Acros Organics	AC392030010	Orange non-toxic drying silicagel
	Desiccant column	*	*	2" dia. clear quartz tube
Data acquisition/ control hardware	Gas sensor	Vaisala	HPP272	
	Control and acquisition	National Instruments	NI-9203	
	Control and acquisition	National Instruments	NI-9263	
	Control and acquisition	National Instruments	NI cDAQ-9172	
	PID controller	OMEGA	CN76000	
	Thermocouple	OMEGA	SMP-HT-K-6	Type K surface probe
	Power supply	ICP DAS USA	DP-640	
	Solid state relay	COSMO electronics corp.	KSD215AC8	
Enclosure	Air-tight enclosure	Pelican	0500 Protector Case	
Other	Hydrogen Peroxide	Fisher Scientific	H325-500	30% aqueous solution

It is important to note that these components were selected for their convenient availability, and that reproducing a system with similar capabilities to ours is possible with different parts, so long as the capabilities of the individual components allow for the same operating conditions.

The flash vaporizer was built using the components shown for reasons stated in section 3.3. Two 100W cartridge heaters were used to ensure plentiful thermal energy could be supplied to the system and prevent drops in surface temperature. The copper block and aluminum plate were held securely together with a CPU cooler assembly, with high-conductivity thermal paste increasing conduction between the two parts.

The injection system was controlled by a syringe pump, which precisely set the liquid injection rate. This was hooked up to the injection point by flexible tubing. This injection tube has a very small diameter, setting the droplet volume at approximately $22.4 \mu L$. The height from which the droplets fell, which affected impact velocity, was controlled by a custom-made 3D printed tube holder.

The fan used in the blower system was chosen for its relatively high static pressure increase (over 5000 Pa) and small size, allowing enough flow through the desiccant to dry the atmosphere at a sufficient pace. A high static pressure increase was important since the packed bed of desiccant beads resulted in a high pressure difference, and less powerful fans, such as computer fans, were not sufficient to overcome it.

The data acquisition and control hardware was chosen based on availability in our campus facilities. A custom LabVIEW software was used to monitor and control all values, except for plate temperature which was set on the PID controller own system.

A large pelican case was used for the enclosure, chosen for its hermetic properties, excellent durability and its large capacity of 267 litres. The only modifications made to it were two small holes; The first served for the flexible tubing to be passed through, allowing the peroxide to be injected from the syringe pump which was kept outside. A tight fit ensured no leak. The second hole was used to pass wires used for the thermocouple, heaters, fan and gas sensor. Silicone was used to hermetically seal the hole around the wires.

3.6 Results

The results acquired throughout this project were submitted to the **HardwareX** journal, published by Elsevier. In line with the open source aspect of this project, this open access journal aims to make scientific hardware open source, building a library of "open hardware". Our designs, software, methodology and results are included in the paper, along with comprehensive Bills of Materials. This is done in the hopes of making it reproducible to mostly anyone worldwide, at a greatly lowered cost compared to commercial alternatives. The article is available in the following chapter.

CHAPTER 4 ARTICLE 1: CONSTRUCTION AND VALIDATION OF AN AFFORDABLE HYDROGEN PEROXIDE VAPOR DECONTAMINATION SYSTEM

Mathieu Chartray-Pronovost ¹, Étienne Robert ¹

¹Polytechnique Montréal, Montréal, Canada

Submitted to **HardwareX** journal

Date of submission: September 10th 2022

Abstract

Due to the COVID-19 pandemic, a sharp increase in the demand for single-use personal protective equipment (PPE) led to a global shortage, increasing exposure of healthcare workers to the virus. Finding ways to reuse such equipment is a critical factor in minimizing the risk of future PPE shortages. Vapourized hydrogen peroxide (VHP) decontamination has been demonstrated to effectively disinfect single-use PPE without damaging it or degrading its efficiency. An affordable prototype relying on mostly commercial off-the-shelf (COTS) components was built using this principle and was able to generate, contain and sustain an atmosphere with a high concentration of H₂O₂. Using a liquid solution of 30% hydrogen peroxide, a flash vaporization technique was used to obtain a stable gaseous H₂O₂ concentration of 500 ppm. A drying system kept the relative saturation well below the condensation point. This allowed precise decontamination protocols to be implemented and tested on single-use PPE at a small flow rate, achieving 6-log reduction of pathogens in a complete cycle with a duration of 2 hours.

4.1 Introduction

The COVID-19 pandemic has led to many problems in healthcare, such as shortages of personal protective equipment (PPE) in hospitals caused by equipment supply problems [26]. This can result in inadequate protection of healthcare workers in a time when they most need it, and subsequently take them out of the workforce if they get infected. Some PPE are single-use, and as such a constant supply must be provided to ensure availability. An important item that suffered critical supply issues during the pandemic are N95 filtering facepiece respirators. These are especially important to counter respiratory diseases such

as COVID-19, since they filter at least 95% of airborne particles. Manufacturers do not recommend reusing these respirators, but authorities such as the United States' Center for Disease Control and Prevention (CDC) may authorize it during crises. To reduce shortage problems, the possibility of their decontamination has been investigated. Depending on the disinfection method, they can safely be used up to 50 times before losing their protective capacities or structural integrity [40]. Disinfection methods commonly used for this kind of equipment are based on hydrogen peroxide (H_2O_2), using either the vapour form of hydrogen peroxide (vH_2O_2), or an atomization process [41]. An advantage of hydrogen peroxide as a disinfecting reagent is that it leaves no toxic by-product, instead decomposing to oxygen and water. H_2O_2 -based decontamination systems are typically quite efficient at removing a broad spectrum of microbes, viruses and fungi [35], but they are expensive and can take months before delivery is completed, meaning smaller or temporary clinics may not have access to them [33]. The objective of the work presented here is to assess the feasibility of building small scale versions of these systems essentially from commercial off-the-shelf (COTS) components, and investigate if such affordable disinfection system are capable of processing PPE for reuse, focusing on N95 masks.

Disinfecting effects and uses

Hydrogen peroxide is a very effective substance for decontamination, often used as a broad-spectrum antimicrobial agent, antiseptic, disinfectant and sterilant [61]. In aqueous solution, it is a staple in healthcare settings for surface disinfection. At low concentrations, usually around 3%, it presents very little risk to cleaning staff, while still being a potent disinfection reagent. Its vapour form is now a widely accepted disinfection tool for sensitive equipment and sealed rooms. However, the high cost and stringent safety measures associated with vapourized hydrogen peroxide mean that such tools are not broadly available outside of major healthcare centers.

The decontamination efficiency of hydrogen peroxide vapour has been widely studied, and its properties are well known. Its mechanisms as a biocide have been extensively studied, and its mode of action both as a gas and a liquid are well understood [85]. Key results reveal it functions by oxidizing susceptible molecular groups that form part of cell walls or intra-cellular components, leading to cell death in microorganisms. It is a powerful sterilant, and is a preferred choice for use where non-toxic by-products are required [57]. Following H_2O_2 decomposition, the only products left after decontamination are water and oxygen.

Decontamination systems

Decontamination systems that use hydrogen peroxide as their primary disinfecting agent may either use it in its liquid, aerosolized or gaseous form. For N95 respirator decontamination, it is recommended to use gaseous hydrogen peroxide, as it offers excellent decontamination efficiency while preserving the longevity of the mask [86]. Submersion in a liquid hydrogen peroxide solution or exposure to aerosolized H_2O_2 has not been demonstrated as an effective decontamination approach, as it is unknown if the hydrogen peroxide can penetrate through the hydrophobic layers of the N95 respirators [66]. Existing cleaning protocols using gaseous hydrogen peroxide either rely on equipment designed to sterilize surgical equipment (Steris V-Pro) to process small batches, or use vapour generators capable of processing whole rooms (Bioquell Clarus) filled with PPE. While the application is different, the principle is similar in both cases and the acquisition cost of such systems is very high (from 20k to upwards of 100k USD). Using these machines, an environment containing a high concentration of gaseous hydrogen peroxide is created and maintained during several minutes to allow the destruction of pathogens. Following proper aeration of the equipment to eliminate leftover peroxide, the PPE is ready to be reused. Gaseous concentration of hydrogen peroxide depends on the manufacturer, with cleaning cycles ranging from 500 ppm to 5700 ppm [65], all achieving satisfactory 6-log reduction of pathogens. Moreover, some systems operate on a dry gas basis, removing water vapour from the atmosphere to prevent condensation, while others do not. There is no consensus in the literature as to whether condensation should be avoided or encouraged [68]. It is up to the customer to determine if their disinfection load is more suited for a dry process or not.

There is a need for decontamination systems in lower resource settings, but research must be done to ensure such systems are efficient, reliable and effective. Operating parameters for a small scale version of commercial systems, built using standard components, are investigated here. The effects of these parameters on the decontamination cycle must be well understood to promote the open source aspect of this project, and make it possible to use different components to achieve similar results.

4.2 Methodology

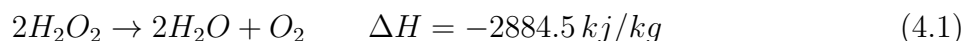
4.2.1 Production of H_2O_2 decontaminating atmosphere

Two main methods exist to generate an atmosphere of gaseous hydrogen peroxide in the context of decontamination. They are evaporation and flash vaporization. While both are based on the phase change of liquid to gas, key differences in the process can yield different

results when used with hydrogen peroxide.

Hydrogen peroxide

Hydrogen peroxide (H_2O_2) decomposes into water and oxygen at standard temperature, with many factors affecting reaction rate, such as temperature, pH, presence of catalysts and even the decomposition environment's volume, surface and geometry [47]. The decomposition reaction is exothermic and can be self-sustaining once it has been initiated. H_2O_2 is considered thermodynamically unstable, with a negative enthalpy of 2884.5 kJ/kg, as indicated in equation 4.1.



Hydrogen peroxide is a strong oxidizer and a reducing agent, due to its oxygen atoms being in a state of reduction [48]. Because of this, hydrogen peroxide reacts with many materials, notably most metals and organic matter. Peroxide can oxidize proteins, lipids and DNA, and is therefore toxic even in small doses.

Many catalysts are effective to break down hydrogen peroxide. Metals are often used in industrial processes because of their efficiency and availability. Hydrogen peroxide also reacts to UV light, making photocatalytic decomposition possible. This means hydrogen peroxide must be kept away from sunlight for storage, lest it naturally decompose.

Evaporation vs Flash vaporization

To obtain a high concentration of gaseous hydrogen peroxide, simply evaporating a liquid solution of aqueous hydrogen peroxide does not suffice. This is due to hydrogen peroxide having a much lower vapour pressure than water, making the latter evaporate first and fill the atmosphere preferentially. Table 4.1 shows the result of evaporating a liquid with a given concentration of H_2O_2 . At equilibrium, the concentration of H_2O_2 in the gas phase will always be significantly lower than that of the liquid.

The equation governing this process is Raoult's law, detailed in equation 4.2.

$$p = \gamma_w p_w^* x_w + \gamma_H p_H^* x_H \quad (4.2)$$

where p is the vapour pressure of the solution, p_i^* the component's vapour pressure, x_i is the mole fraction of the component in the solution, and γ_i is the activity coefficient of the component. Subscripts W and H refer to water and hydrogen peroxide respectively.

Liquid (% w/v)	Vapour (% w/v)
32.1	1.87
55.7	8.0
73.9	24.1
77.8	35
88.3	56.4

Table 4.1 Equilibrium concentrations of H_2O_2 vapour over liquid H_2O_2 at $t = 25$ °C [61]

A higher H_2O_2 concentration in the liquid solution could increase the vapour concentration, but there are many risks associated with high concentrations of liquid hydrogen peroxide. For safety reasons, concentrations above 50% are rarely used. Moreover, because of Raoult's law, the concentration of H_2O_2 in the liquid solution will gradually increase as evaporation progresses, since water evaporates preferentially. This can cause an originally safe solution to become dangerous.

An important parameter for H_2O_2 systems is the relative saturation, which is the combined humidity of water vapour and hydrogen peroxide vapour. At 100% relative saturation, condensation occurs, forming potentially dangerous high concentration H_2O_2 droplets, even if the atmosphere is not saturated when considering the water or H_2O_2 alone.

To circumvent the limitations imposed by Raoult's law, a technique called flash vaporization is often used [79]. This consists of rapid evaporation of small droplets of the liquid solution on a hot plate whose temperature is much higher than the boiling point of the solution. This ensures that all H_2O_2 is turned into vapour. Before equilibrium is reached, the atmosphere must be dried, else the result is the same as normal evaporation. This is done in a loop, as explained in section 4.2.2.

Challenges

Because of its properties, working with hydrogen peroxide vapour to produce a consistent and stable high concentration can prove difficult. The presence of catalysts in the decontamination chamber will start the self-sustaining decomposition reaction, eventually leaving nothing but water and oxygen. Chamber materials and geometry must therefore be chosen carefully to prevent unwanted decomposition. Even usually nonreactive materials such as 304 stainless steel [76] and titanium can be oxidized by hydrogen peroxide, and their use must be restricted [54]. Some polymers are completely nonreactive, but their mechanical properties and longevity can make them sub-optimal for certain applications. A mix of both metals and polymers can be used to take advantage of the best properties of both types of materials. In our case, a polypropylene enclosure was used, with ABS plastic and aluminum

used for internal components to ensure the lowest possible catalytic activity.

Because of the low Permissible Exposure Limit (PEL) for hydrogen peroxide vapour (1 ppm) [60], care must be taken to ensure the enclosure is gastight. Moreover, proper aeration must be available to rid the equipment of any residual peroxide before it is taken out of the enclosure. The concentration of gaseous hydrogen peroxide must therefore be carefully monitored, both to ensure it meets the decontamination requirements, and that it becomes sufficiently low at the cycle's end.

The relative saturation of the enclosure's atmosphere must also be monitored, as it provides information on condensation. Since the target equipment to be decontaminated by this system is N95 respirators, condensation should be avoided, as it could interfere with the filter's properties and lower its efficiency.

Since it is not always practical or feasible to thoroughly remove all chamber contaminants, and since the decontamination load may vary, some H_2O_2 decomposition always occurs. Therefore, in order to maintain a concentration sufficiently high to guarantee decontamination, hydrogen peroxide vapour must be continually fed into the system.

Additionally, since water is present in the feedstock, and is also created during the decomposition process, humidity will rise until the chamber is completely saturated in water. The process must therefore include a method of drying the atmosphere.

4.2.2 H_2O_2 vapour generator

The hydrogen peroxide gas is generated by a flash vaporizer in order to circumvent limitations that would be imposed by Raoult's law. The atmosphere inside the enclosure is continuously dried to prevent condensation. The components used are detailed in this section.

Closed loop design

To ensure a high concentration of gaseous hydrogen peroxide while preventing condensation, a closed loop design is typically used in decontamination systems [68]. A single closed loop was used for this project, to reduce complexity and ultimately enable the components to be packaged in a shoebox-sized case, such that it could theoretically be placed in any gastight enclosure and transform it into a decontamination system. The main components of such a design are shown in figure 4.1.

A gastight travel case (Pelican 0500) was used as the decontamination enclosure for the results presented here. This enclosure was chosen since it is completely hermetic, and is also

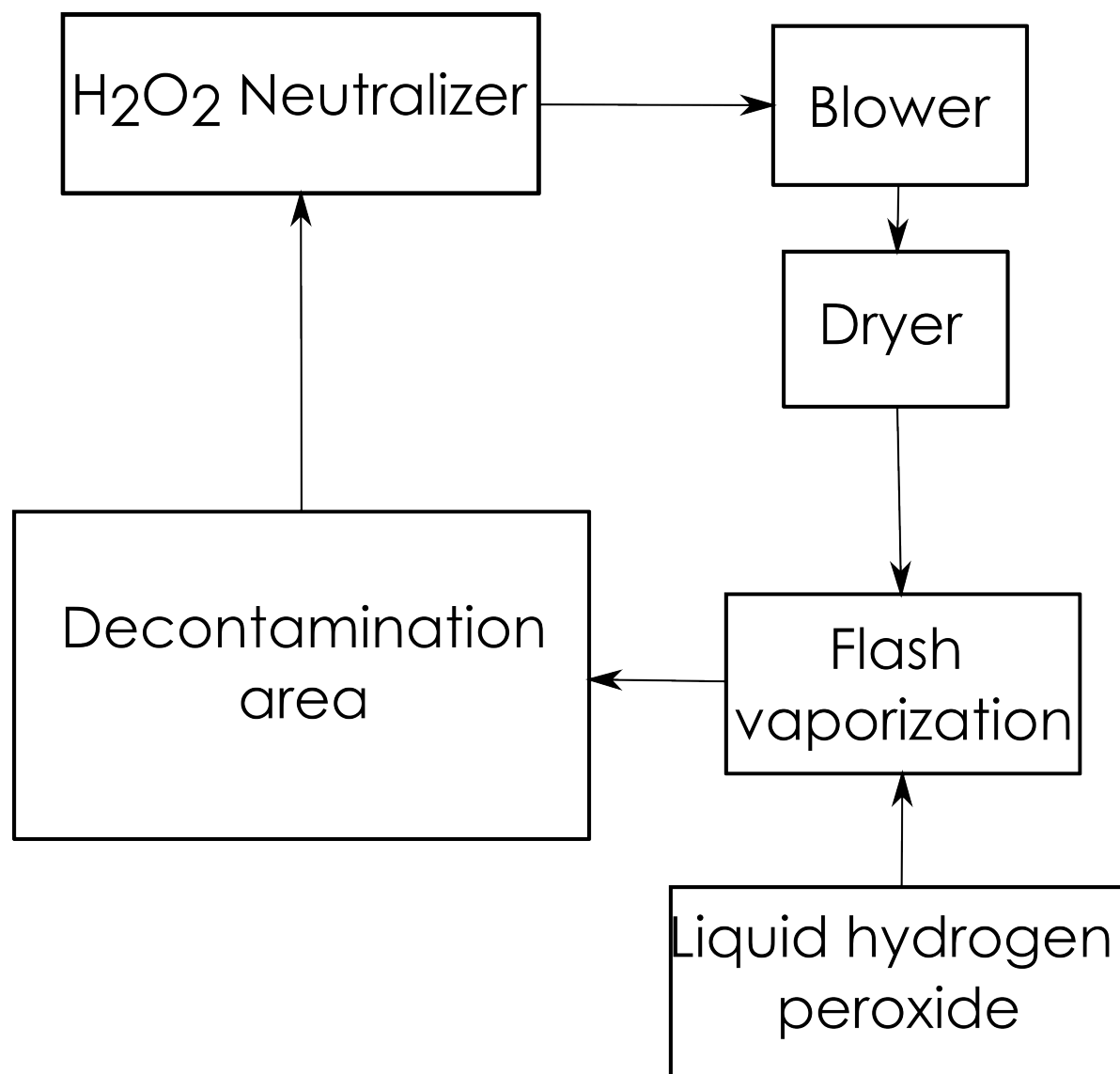


Figure 4.1 Closed loop system schematic

non reactive with hydrogen peroxide, being made mainly of polypropylene. This ensures user safety, as well as efficient decontamination.

The H_2O_2 vapour sensor is located within the decontamination area, and continuously monitors concentration as well as relative saturation. Together with data acquisition hardware and software located outside the enclosure, this forms a secondary control and monitoring loop. A Vaisala HPP272 probe is used as a vapour sensor, while National Instruments (NI) cards are used together with the labVIEW software for data acquisition. An ATI 00-1169 H_2O_2 gas sensor was also used in conjunction with the Vaisala sensor for some tests, to ensure proper monitoring. The custom software used is available in a public github repository for this project,

along with the parts list and custom designs: <https://github.com/mathiforce/open-VHP>

Flash vaporizer

The component used for the creation of hydrogen peroxide vapour is called the flash vaporizer. It is an assembly of parts that serves to rapidly heat up droplets of the liquid solution of hydrogen peroxide. It consists of an aluminum plate, a heated block of copper, cartridge heaters, a bracket assembly, a type K thermocouple, an OMEGA CN76000 PID controller and an injection tube.

The liquid solution is injected through a 0.85mm-thick tube, with the rate precisely controlled with a New Era NE-4000 syringe pump. The droplets fall onto the plate, whose surface temperature is kept well above the boiling point of the solution. This plate is made of aluminum, chosen for its low reactivity with hydrogen peroxide, and its high thermal conductivity. It is maintained firmly in contact with a block of copper, with thermal paste connecting the two. This block serves as a heat buffer, since copper has high density and thermal conductivity. This buffer makes the flash vaporizing more consistent, as more thermal energy is readily available, reducing the importance of fluctuations in surface temperature caused by the droplet evaporation. Copper cannot be used for the contact plate itself, since it is highly reactive with H_2O_2 . The block of copper is heated by two cartridge heaters, delivering a combined maximum power of 200W. This is ample power to maintain the surface at a high temperature, accounting for the energy necessary for the vaporization of the solution and losses to the surrounding.

The temperature is measured with a type K surface probe thermocouple, which feeds its value to a PID controller. This controller is also connected to the cartridge heaters, in a feedback loop that enables reliable control of the surface temperature within the precision of the controller, or approximately $\pm 1^\circ\text{C}$.

The diameter of the injection tube was chosen to be as small as possible. With an external diameter of 0.85mm, this results in droplets of approximately $22.4\mu\text{L}$ in volume. The goal was to make the droplets very small to evaporate them quickly and therefore prevent thermal decomposition in the droplets, which could be exacerbated by longer contact with the hot plate, as well as the rise in concentration as the droplet evaporates. A low injection rate ensures that individual droplets form and fall due to gravity, taking full advantage of the flash vaporization technique.

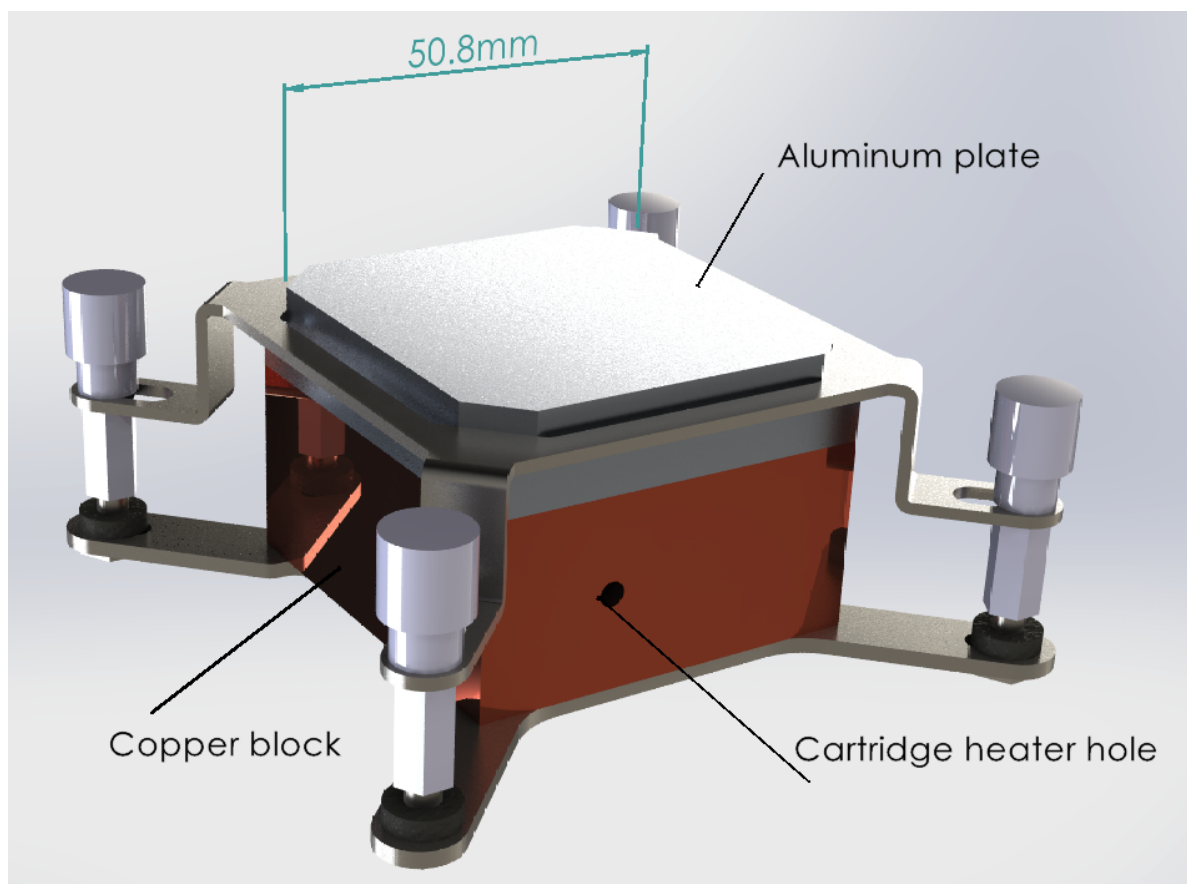


Figure 4.2 Flash vaporizer assembly

Fan-driven desiccant column

The H_2O_2 neutralizer, blower and dryer components of the loop shown in figure 4.1 are combined into a single item, taking the form of a fan-driven desiccant column. This is desirable to simplify the design as there is no use case where it would be necessary to decouple the drying and H_2O_2 neutralization aspects. As such, the desiccant fills both needs in an easy to implement way. The chosen desiccant, silica gel, can also be reused following heating. The atmosphere inside the enclosure is forced through the desiccant column by a centrifugal fan. The hydrogen peroxide is destroyed through a combination of desiccant adsorption and passing through the centrifugal fan, triggering decomposition. The water vapour is removed from the atmosphere in the desiccant.

This component can reliably remove water and H_2O_2 vapour from the enclosure's atmosphere for the complete duration of a cycle, typically on the order of 2 to 4 hours. For consistency and safety considerations, it is recommended to replace the desiccant with a dry batch after each test. In future work, a heating system could be implemented to regenerate the desiccant

internally.

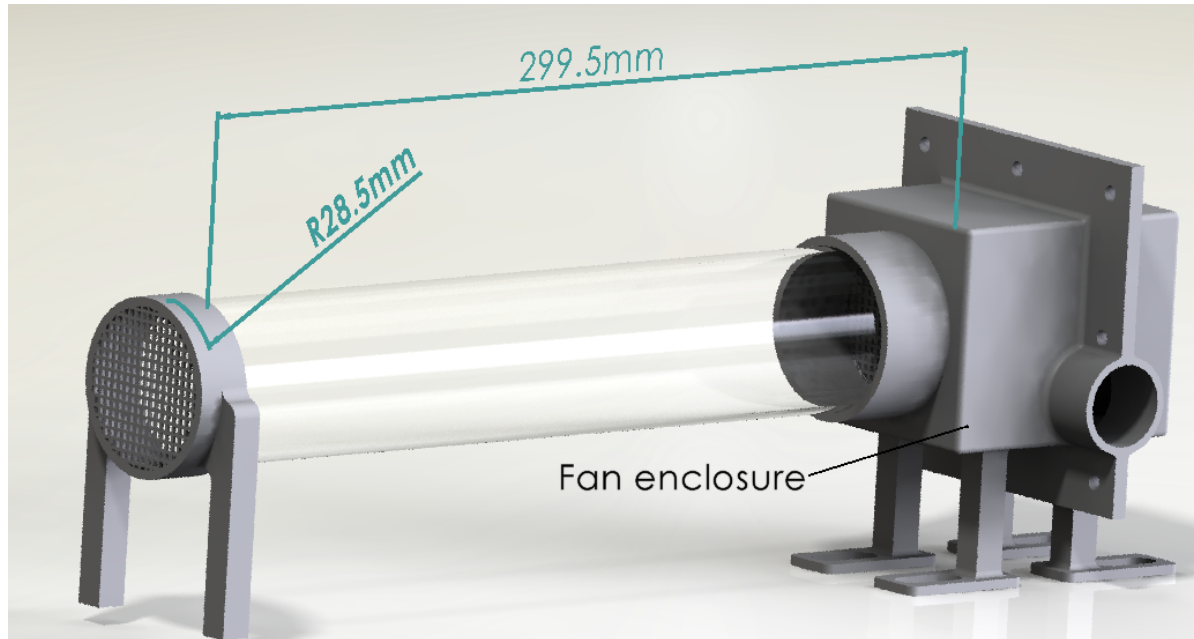


Figure 4.3 Powered desiccant column (silicagel not shown)

Biological indicator

Bacterial spores were used as biological indicators since they can be difficult to sterilize, and are therefore often used to assess the decontamination efficiency of similar systems. *Bacillus Subtilis* spores were used for their well-researched properties in the literature and their local availability [87]. They can form a protective endospore which can render sterilization difficult, making them highly resistant and therefore a proper test of our system's possibilities.

These spores were inoculated on coupons, which were cut sections of a N95 respirator (3M 8210). Different mask zones were used to make coupons to verify if some areas were more difficult to sterilize. These coupons were then placed on a holder inside the enclosure and processed. Following a complete cycle, the spores were incubated for 24 hours and the colonies counted.

Decontamination cycle

The cycle used for decontamination was based upon our own work with the system, along with literature baselines. It consists of four phases, after which the equipment is ready to be taken out, and biological indicators can be processed.

In the first phase, the atmosphere in the enclosure is prepared, mainly through drying. This goes on until the limit of the drying device is reached, at approximately 10% relative saturation in our case, from 25-30% under ambient conditions. Once this is achieved, the second phase starts. This is the atmosphere conditioning phase, where liquid hydrogen peroxide is injected and vaporized until the desired gaseous concentration is reached. Based on a report by Battelle [40], this value was chosen as 500 ppm. As soon as this value is reached, the main phase begins, namely sterilization. The concentration is kept constant in the chamber, and relative saturation is monitored to ensure it does not reach values that would permit condensation. This phase lasts for a set amount of time, and 30 minutes were found to be sufficient to obtain the results shown in section 4.3. After this time has passed, the injection is turned off and the desiccant column is allowed to get rid of the hydrogen peroxide in the enclosure. This aerating phase lasts the longest, since the gaseous concentration must be below the PEL for H₂O₂ at 1 ppm.

Depending on the length of the first and last phases, which may vary according to initial conditions, decontamination load and desiccant state, the whole process may take from 2 to 4 hours.

Evaporation efficiency

Evaporation efficiency was defined as followed:

$$\eta_{evap} = \frac{\dot{m}_g}{\dot{m}_l} \quad (4.3)$$

where \dot{m}_g and \dot{m}_l are the mass flows of gaseous and liquid hydrogen peroxide to the system, respectively. This represents the fraction of hydrogen peroxide that is successfully evaporated. The difference between these two mass flow values represents the quantity of hydrogen peroxide that is lost between the flash vaporization device and the gaseous H₂O₂ sensor.

\dot{m}_l is a control parameter of our experiments, set by the syringe pump. It is therefore known and assumed constant. \dot{m}_g is calculated from the test results. Since the system is continually destroying the gaseous hydrogen peroxide to keep the relative saturation low, \dot{m}_g cannot be calculated simply from the liquid injection flow rate. The value read by the H₂O₂ sensor represents the total mass flow of all combined production and destruction effects, as follows:

$$\dot{m}_t = \dot{m}_g - \dot{m}_d \quad (4.4)$$

where \dot{m}_t is the total mass flow and \dot{m}_d is the rate of destruction of gaseous H₂O₂. \dot{m}_d is itself composed of all mechanisms that reduce the gaseous concentration in the enclosure, such as the destroyer-dryer-blower device, thermal decomposition and condensation of hydrogen peroxide. However, as explained in section 4.3, the component mainly responsible for H₂O₂ destruction, by a large margin, is the destroyer-dryer-blower device. It is possible to isolate this parameter during the drying phase of a typical test, where no liquid hydrogen peroxide is injected, but the destroyer-dryer-blower device runs until the gaseous concentration reaches a sufficiently low value that is considered safe for opening of the enclosure ($< 1ppm$).

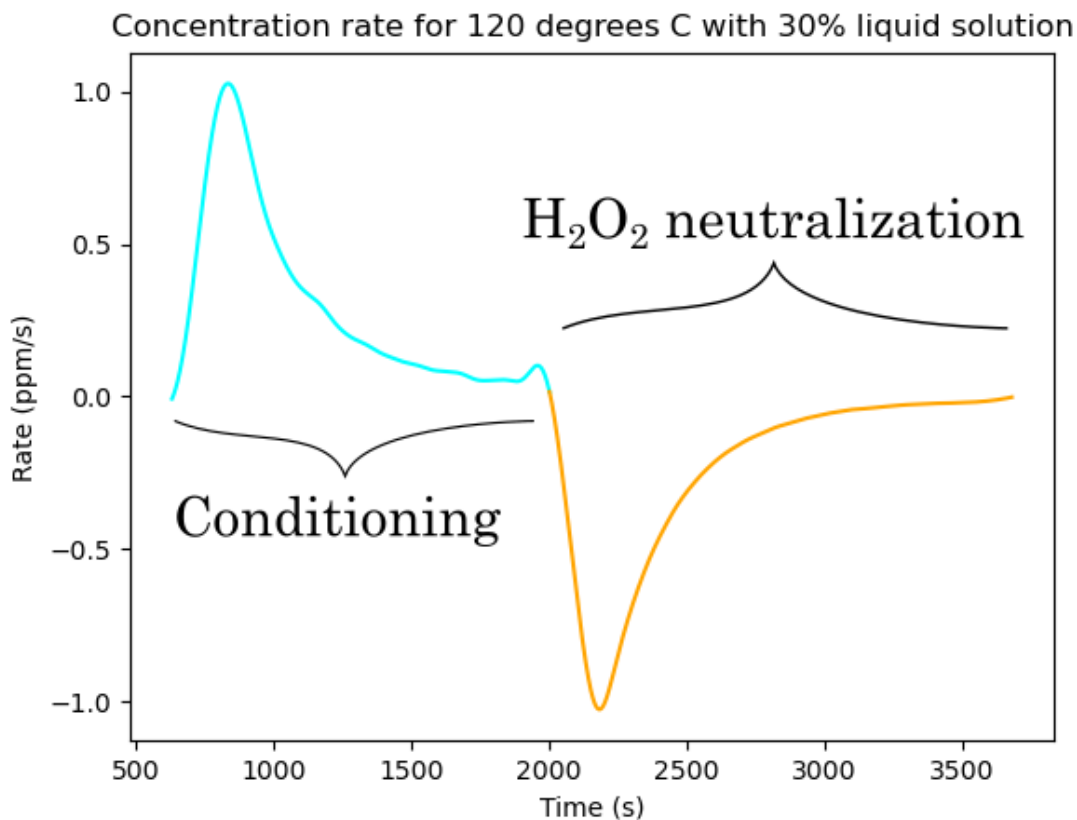


Figure 4.4 Typical concentration rates for injection and drying phases

\dot{m}_d is calculated by numerical integration of the test data. This gives the total mass of hydrogen peroxide involved in both test phases, as shown in figure 4.4 for a specific test. This value is then divided by the phase's duration to obtain an average mass flow. This method is used to obtain an estimation of the average mass flow that is independent of the test duration. Knowing \dot{m}_t and \dot{m}_d , \dot{m}_g is then calculated, and compared to \dot{m}_l to obtain the

evaporation efficiency.

4.3 Results

4.3.1 Cycle concentration and saturation

Tests were done at different injection flow rates and a constant plate temperature of 110°C, with the results available in figure 4.5. These tests were used to determine the flow rate necessary to obtain 500 ppm during the decontamination tests.

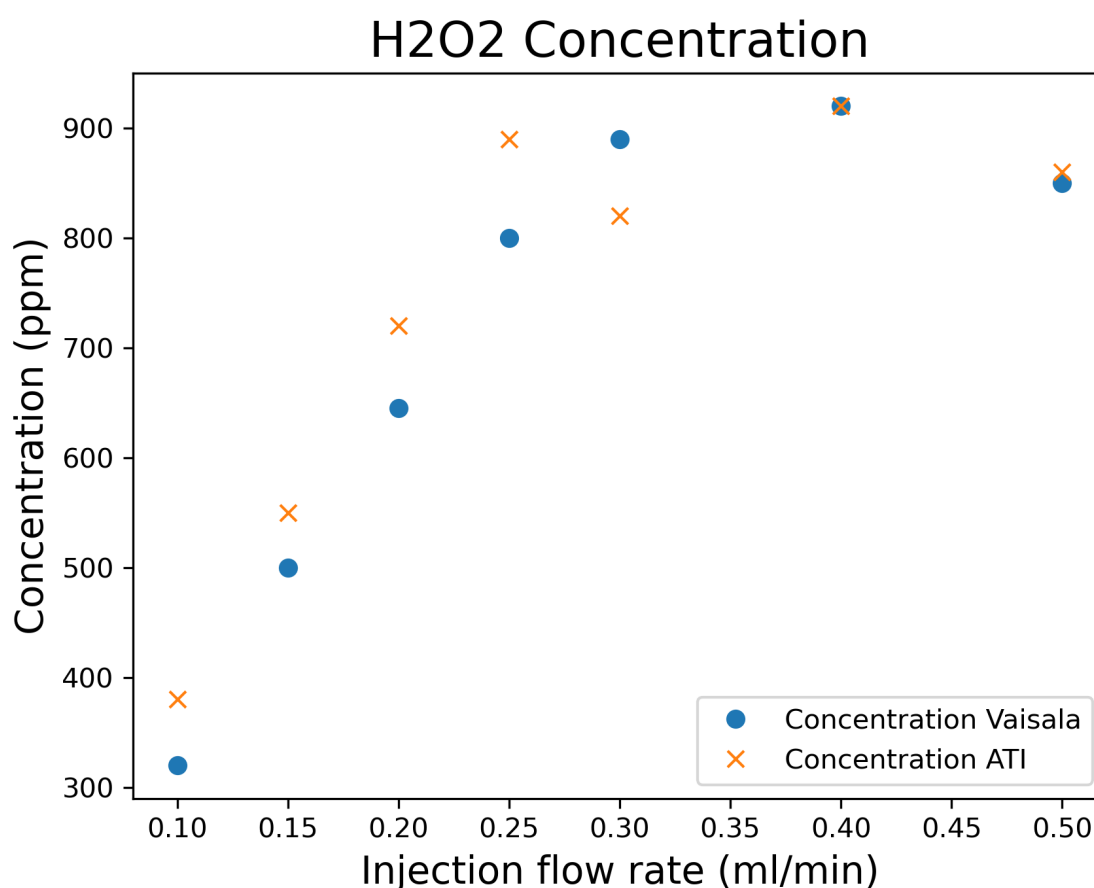


Figure 4.5 Peak concentration vs. injection flow rate

The two different gaseous H_2O_2 detectors were used to measure the maximum concentration values. Both detectors gave similar results, with a value of approximately 50 ppm separating the two. We can observe a mostly linear increase trend for the maximum value of the H_2O_2 concentration in the injection enclosure as a function of flow rate. Above 0.3 ml/min for a

plate temperature of 110°C, a plateau in the maximum gas concentration is reached. This is due to the fact that the droplets come too quickly for the flash vaporizer to keep up, and the excess is either accumulated or decomposed. The maximum value attainable by varying only the flow rate at this temperature is just above 900 ppm for a H_2O_2 solution of 30%.

The following results were gathered during the decontamination cycles where inoculated test samples of N95 respirator were placed in the enclosure. Only two such full tests were completed, but the repeatability of the concentration measurement was assessed through several other tests. The desired concentration of 500 ppm was successfully attained and maintained for 30 minutes during all tests, using a liquid flow rate of 0.15 ml/min. Initial relative saturation varied between 25% and 30%, and was lowered to approximately 10% prior to H_2O_2 injection. The maximum value for relative saturation was reached at the end of the sterilization phase, and ranged from 30% to 50%.

H2O2 vapor concentration and relative saturation

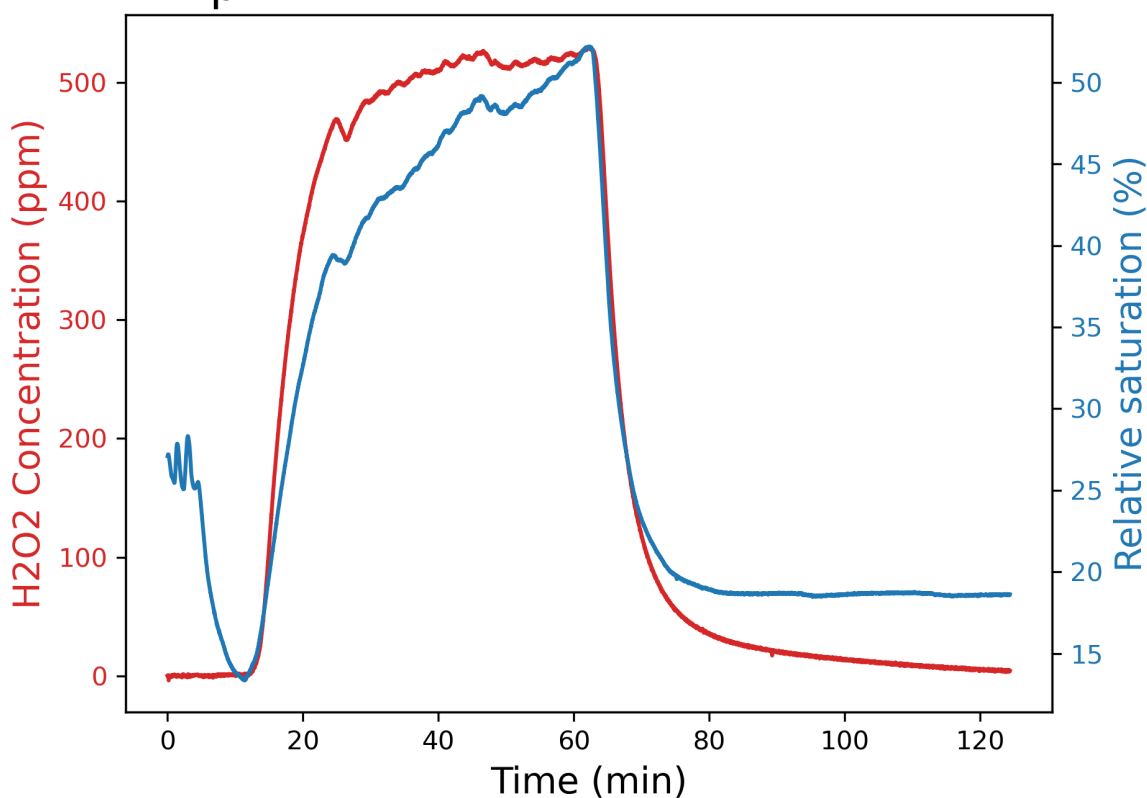


Figure 4.6 Concentration and relative saturation during test

Figure 4.6 shows the values of gaseous H_2O_2 concentration and relative saturation during the whole decontamination process. Following a rapid rise, the value of concentration stabilizes

at approximately 500 ppm until injection is stopped, while saturation continues increasing after the initial rise, albeit at a slower rate. Both values drop very quickly once the sterilization phase is complete, with saturation reaching its final stable value after approximately 20 minutes. It takes more than an hour for the gaseous concentration of hydrogen peroxide to drop below 1 ppm.

4.3.2 Pathogen reduction

Five droplets of 2 μL each were deposited onto each coupon, for a total of 10 μL of *Bacillus Subtilis* spore solutions. With the mother solution having a concentration of $10^{8.9}$ spores/ml, this resulted in each coupon being inoculated with $10^{6.9}$ spores.

Test #	Volume	Initial spores quantity	Final spore quantity	Reduction
Test 1	10 μL	$10^{6.9}$	0	6.9 log
Test 2	10 μL	$10^{6.9}$	0	6.9 log
Control	10 μL	$10^{6.48}$ and $10^{6.78}$	3 and 6	0

Following decontamination and incubation, no spores had formed colonies from the coupons that were processed. Colonies were still formed from a control group of the same spore solution that was not decontaminated. From the final spore quantity found by counting the colonies of the control petri dishes, which were 10^{-6} dilutions, we find that initial spore quantity was between $10^{6.48}$ and $10^{6.78}$ for the control, near the value of reference given by the mother-solution. This results in the system being able to achieve at least approximately a 6.9 log reduction in *Bacillus Subtilis* spores.

4.3.3 Evaporation efficiency

The trends resulting from the tests on evaporation efficiency closely follow what is expected from the literature, as can be seen in figures 4.7 and 4.8.

As explained in section 4.2.1, it is expected that a higher concentration in the liquid solution will also lead to a higher proportion of gaseous hydrogen peroxide in the vapour headspace, in a non-linear fashion. Figure 4.7 shows the evaporation efficiency increasing in a similar fashion, since it is affected by the liquid concentration. However, as the plate temperature is increased beyond a critical value, the efficiency drastically decreases, as shown by figure 4.8.

The evaporation efficiency as a function of temperature reveals two trends, on either side of this critical temperature. Before this point, efficiency seems to increase as temperature does. However, once past this point, the opposite is true, with efficiency decreasing sharply with

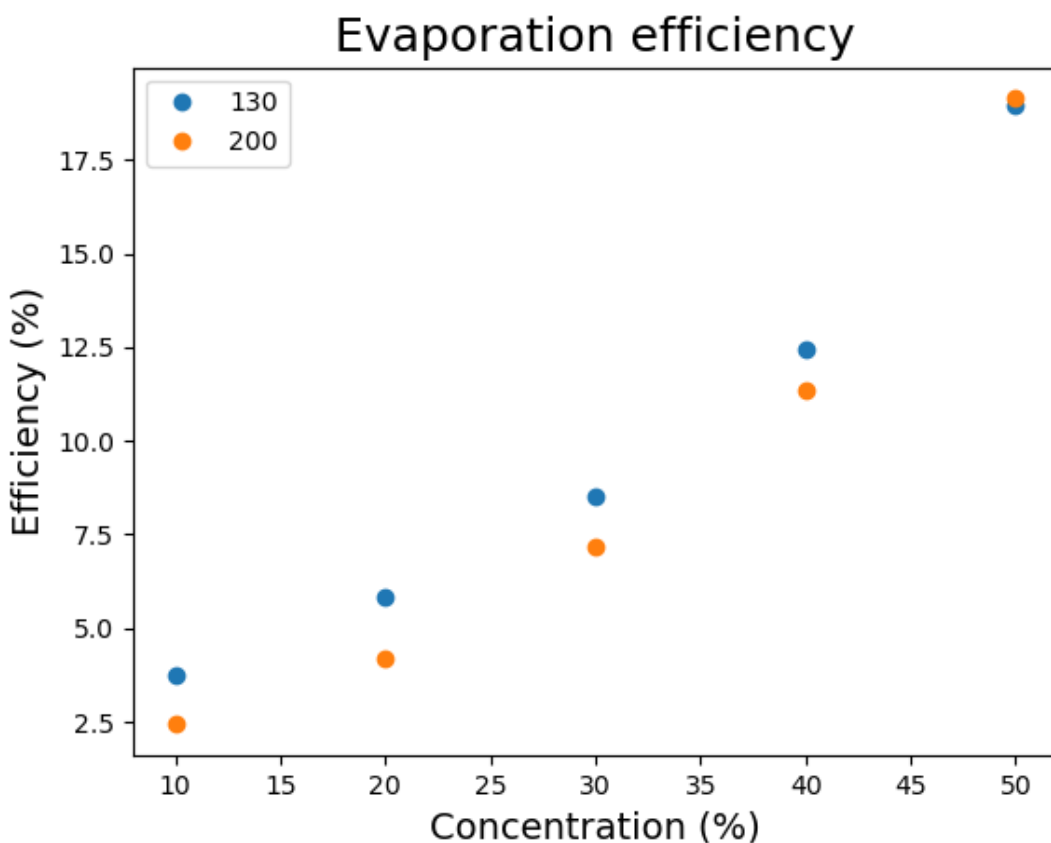


Figure 4.7 Evaporation efficiency at constant temperature

increases in temperature. The maximum efficiency is found at the intersection between these two curves, at said critical temperature. The causes for this transition, as well as overall system performance, are discussed below.

4.4 Discussion

Supply issues were quite severe during some periods of the COVID-19 pandemic, leading to extreme scarcity of N95 respirators for healthcare personnel. Outside of large healthcare centers, there are few systems available for PPE decontamination. Since such systems are complex and expensive, a novel approach was tested that consisted of building a decontamination system using vapourized hydrogen peroxide, in an affordable and easily reproducible way. Through our decontamination tests, we have demonstrated that it is possible to successfully build such a system and disinfect N95 respirators.

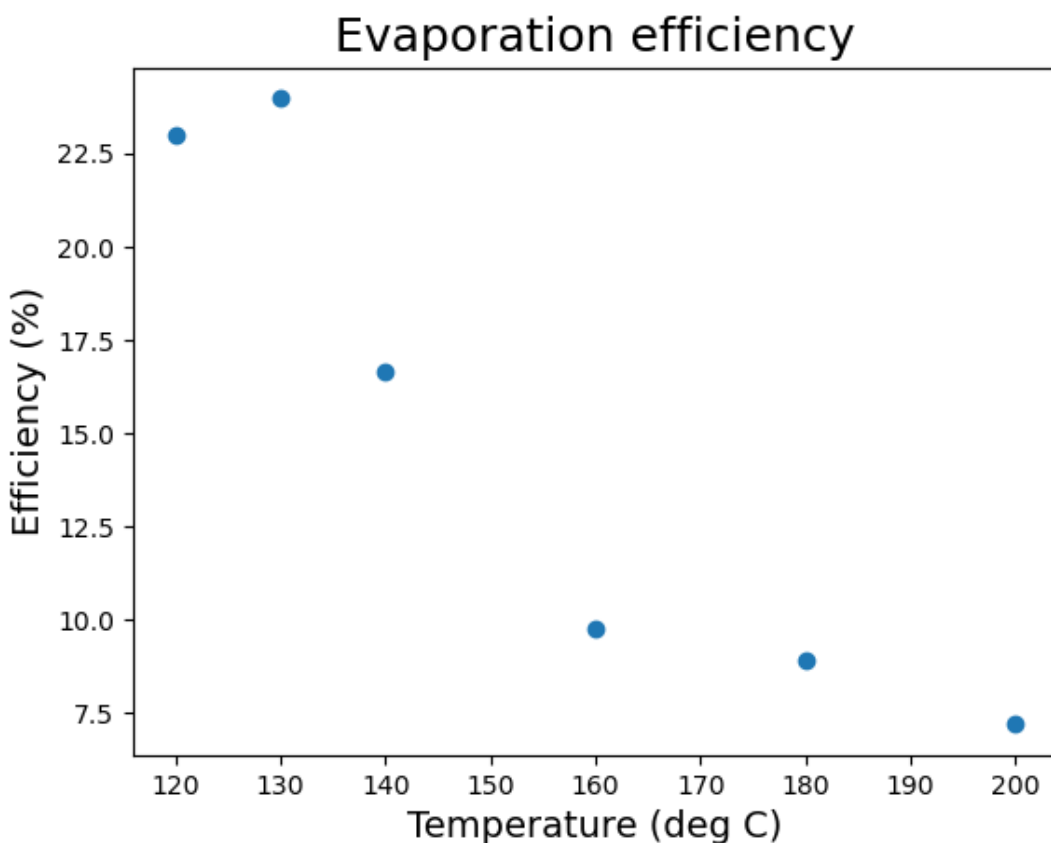


Figure 4.8 Evaporation efficiency at constant concentration

4.4.1 Cycle Reliability

Our decontamination tests, and assessment of the effect of the injection flow rate showed that the system built shows good reliability. It is expected that as long as the equipment processed is similar to our benchmark N95 masks, it will be successfully disinfected after the cycle implemented. A 6.9 log reduction of *Bacillus Subtilis* spores was achieved with our system. The biggest source for potential differences in test results seems to be the state of the desiccant in the powered desiccant column. If a desiccant with very different properties is used, or if the desiccant is not dried between cycles, results could potentially vary. Indeed, figure 4.6 shows that the drying system is less effective after a cycle, with a relative saturation approximately 5% higher than the initial value. Since removing the water vapour in the enclosure's atmosphere is crucial to the system's operation, the desiccant must be in its most efficient state at the cycle's start.

Bumps can be seen at a regular interval in the concentration and saturation values during a

test. This is due to the flash vaporizer being a dropwise device. The drops must be separated in time in order for the heated surface to recover its optimal temperature and keep the flash vaporization efficient.

A sustained H_2O_2 concentration value of 500 ppm was sufficient to decontaminate N95 respirators, but it is possible to reach values above 900 ppm with the system, as built. Increasing this maximum value further would require either a more concentrated liquid solution, different vaporizer geometry or a different dryer or H_2O_2 neutralization stage. This might be useful to consider if different equipment are to be treated, since some materials might need a higher concentration in order to successfully be disinfected.

4.4.2 System efficiency

The tests done to find the evaporation efficiency at various operating conditions were useful to determine where the system most efficiently transforms the liquid hydrogen peroxide solution into H_2O_2 vapour. Indeed, the properties of H_2O_2 , notably its thermal decomposition, make the system sensitive to the temperature of the hot plate. Coupled with the complex geometry of the enclosure, high vaporization temperatures and the possibility of condensation, experimental tests were necessary to quantify the efficiency. Higher liquid concentrations are desirable to obtain the highest efficiency, but the same is not true for temperature. For the latter, maximum efficiency is reached just above the liquid solution's boiling point.

With high-speed imaging, the flash vaporizing device was further analyzed and it was found that high temperatures associated with the emergence of the Leidenfrost effect, which makes the droplets float above the heated surface on a thin layer of vapour. Because of this phenomenon, droplets take considerably longer to vapourize and fragmentation can result in some of the liquid being ejected from the plate. A comparison of droplet behaviour above and below the Leidenfrost is shown in figure 4.9, for a peroxide concentration of 10% and a constant droplet impact velocity between the two tests.

The peroxide in the droplet is also more prone to decomposition because of the progressive rise in temperature. Since small droplets are more likely to move from the Leidenfrost effect [83], the small scale of our system introduces this phenomenon in a way that might not be present in bigger commercial alternatives. The critical surface temperature at which system efficiency is highest is therefore just below the Leidenfrost point, which is unfortunately quite a complex phenomenon, being dependent on the material and its microstructure, in addition to temperature. The exact role of Leidenfrost effect in flash vaporization of H_2O_2 solution is therefore left for future work.

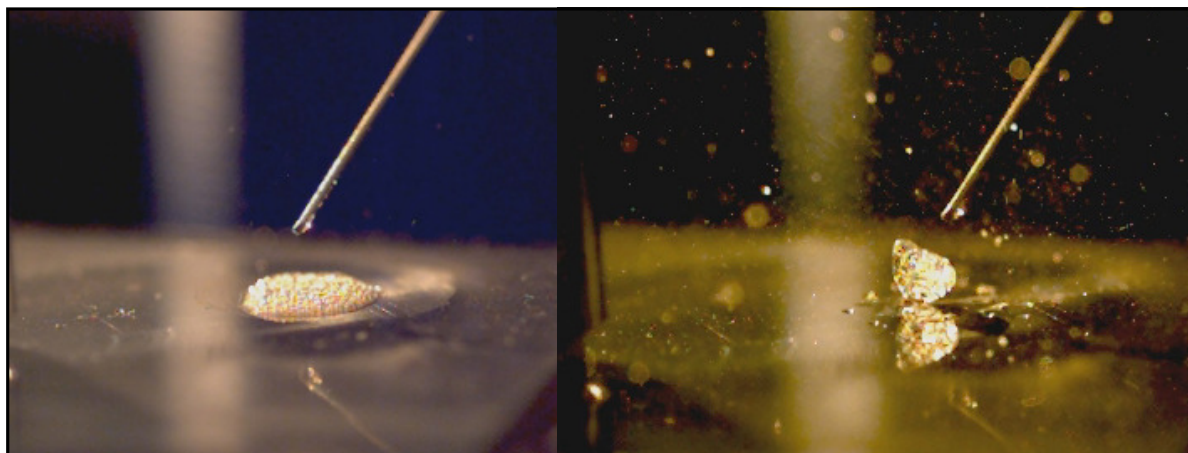


Figure 4.9 Comparison of droplet behaviour below and above the Leidenfrost point

4.5 Conclusion

To summarize, a portable, cost-effective H₂O₂ vapour generator has been shown to successfully disinfect N95 respirators. These PPE, which are traditionally single-use, can therefore see their useful life extended. This can greatly appease supply issues during times of crisis. The system built here can achieve performance similar to commercial alternatives, but the much lower cost make it available to more resource-starved environments, since commercial VHP systems are rarely seen outside of large healthcare centers. The freedom in component choice also makes it possible to build such an affordable system in a much shorter time than would be necessary for the purchase and delivery of a commercial system.

It was found that using a solution of 30% hydrogen peroxide, a temperature of approximately 130°C was optimal for flash vaporization, with a sustained gaseous concentration of 500 ppm reached. An increase in the liquid injection rate can lead to a maximum concentration of approximately 900 ppm, opening the possibility to more potent decontamination without any system modification.

The work presented here is made available open-sourced through a github repository, allowing systems to be built wherever needed, with local components and our own custom part designs and software. Users are free to adapt the systems to their needs, with the guidelines in this article helping obtain a satisfactory level of disinfection through the research done on the various components necessary to build a VHP system.

CHAPTER 5 GENERAL DISCUSSION

Additional discussion can be had that did not necessarily fit the journal article's scope. In a general manner, it was successfully demonstrated that a VHP system can be built using mainly commercial off-the-shelf (COTS) components and 3D printed custom designs. Many different component alternatives can be used to build a similar system, as long as they meet the same specifications. This means that the open source system design is more resistant to supply issues, such as those that appear during times of crisis like pandemics, and it is also more easily available to worldwide countries compared to commercial systems.

More tests would need to be done on the decontamination aspect itself. Real-world cases such as running a cycle with the enclosure packed with as many N95 respirators as possible should be done to ensure H_2O_2 concentration and relative saturation values are similar and sterilization is as effective as our small-scale tests. The additional surface area present during a full-scale test could potentially affect peak H_2O_2 concentration and relative saturation, although this could be taken into account by increasing liquid H_2O_2 mass flow, as results show that peak H_2O_2 concentration can still be increased by increasing this parameter. Mixing of the enclosure's atmosphere might also be affected, and some masks might receive a lesser dose of gaseous H_2O_2 . A proper test with biological indicators placed in strategic locations is necessary to ensure the system can process a full load of equipment.

Nevertheless, our tests show that N95 mask coupons inoculated with bacterial spores are sterilized after a two hour cycle containing a 30 minute sterilization phase. The operating parameters that were found most optimal were not tested with another system, but should be the same for other systems respecting the same specifications. If not, they can be varied to obtain the same results.

A strong dependency between system performance and flash vaporizer plate temperature was found. There is an optimal temperature that is neither too low or too high, situated just below the component's Leidenfrost point. This temperature is therefore the most sensitive parameter, given hydrogen peroxide's properties and the complexity of the Leidenfrost phenomenon.

CHAPTER 6 CONCLUSION AND RECOMMENDATION

6.1 Summary of Works

The work presented here concerns the design, construction and validation of a decontamination system targeted towards personal protective equipment (PPE), more precisely N95 filtering facepiece respirators (FFRs). This system was built using an affordable approach in the hopes that it can easily be reproduced in places where commercial alternatives might be too expensive or otherwise not available. This project was initiated after the COVID-19 pandemic resulted in severe shortages of protection equipment. This shortage put healthcare workers at risk and exacerbated the pandemic's effects on the population, because sick healthcare workers were removed from the workforce. N95 masks are single-use PPE, but the crisis forced workers to reuse them due to lack of new supply. Decontamination of this equipment at least ensures it is sterile upon reuse. However, few healthcare centers outside of main hubs are equipped with the facilities to disinfect these respirators. Commercial decontamination systems that can process N95 masks are expensive, and might not be available for weeks or months after ordering. Lower resource settings might not have the possibility to decontaminate their respirators at all. This is why an open-source and affordable alternative might be beneficial and offer much needed relief to the supply chain in times of crisis, ultimately protecting the health of workers and patients. Such a system could be assembled in temporary clinics when needed, and dismantled when the pandemic surge subsides.

The method identified as the best candidate for FFR decontamination is vaporized hydrogen peroxide (VHP), for its potent decontamination power and capacity to penetrate the porous materials of such respirators. Moreover, such systems have a small footprint and can be contained in relatively small spaces, set largely by the size of the enclosure in which equipment is processed. Based on a technique called flash vaporization, a compact system was designed capable of similar performance to commercial alternatives, for a fraction of the price. The majority of the system was built using locally available components, with some additional ones purchased online, such as the H_2O_2 gas sensor. The system integrates a loop design that continuously dries the atmosphere of water vapour, which is necessary for flash vaporization to be effective and gives the possibility of attaining a high concentration of gaseous H_2O_2 . Using silicagel and an electric fan, this drying loop also acts as a H_2O_2 neutralizer, ridding the atmosphere of residual hydrogen peroxide after the sterilization is complete. This leaves the decontaminated equipment safe to reuse. The commercial H_2O_2 sensor in the enclosure gives real-time monitoring capabilities to the system, using our own data acquisition cards and

software. Parameters such as H_2O_2 concentration and relative saturation are continuously recorded to ensure the necessary values are obtained.

Through numerous tests the system proved to be reliable and consistent. Many parameters were studied in order to operate the system in an efficient manner, in order to use the least resources possible, preserve system integrity and properly disinfect equipment.

An aqueous solution of 30% hydrogen peroxide was used as the liquid reagent, for its relative ease of acquisition, its high potential gaseous concentration and its reduced effect on equipment compared to higher concentrations. With a flow rate of 0.15 ml/min, a gaseous H_2O_2 concentration of 500 ppm can be maintained in the decontamination area for at least 30 minutes, which is sufficient to decontaminate N95 respirators. A surface temperature of 130 °C was found to be optimal for our flash vaporizer design, reducing vaporization time while keeping out of the film boiling regime. Aluminum was used in conjunction with copper for the flash vaporizer, combining the chemical resistance to H_2O_2 of aluminum with the high thermal effusivity of copper.

The final result is a system that can successfully disinfect N95 respirators in approximately 2 hours, achieving over a 6-log reduction in *Bacillus Subtilis* bacterial spores.

6.2 Limitations

While this system might successfully disinfect N95 respirators, the latter only represents a small fraction of PPE that might be used by healthcare personnel on a frequent basis. Tests need to be done on each specific type of equipment to verify its compatibility with the system built here. The testing protocol used for N95 masks, consisting of *B. Subtillis* inoculation as detailed in chapter 4, can be extended to a wide range of equipment. Once an equipment's compatibility has been validated with our system, it would theoretically be compatible with all systems built that can attain the same operating parameters, such as gaseous H_2O_2 concentration and relative saturation.

Another limitation of this project is the inherent dependence of the system's performance on the flash vaporizer. Because of hydrogen peroxide's reactivity and thermal decomposition, the flash vaporizer is the most critical component, directly affecting the potential for creation of an atmosphere of gaseous H_2O_2 . Many aspects of this component can affect its efficiency, such as material, geometry and surface treatment. Using an incompatible material is likely to result in unwanted results, such as low H_2O_2 concentration and degradation of the vaporizer itself.

The system's performance is also dependent on the neutralizer-dryer, although in a less

dramatic manner than the flash vaporizer. The desiccant's state at the beginning of the test determines how much vapour it can absorb, and therefore the relative saturation during the process. Variations in this state might give different results. A way to easily regenerate desiccant could be integrated to the system, as a post-process phase that would return the desiccant to its original state for each cycle, removing a source for error. This could simply be a heating element that would heat air passed over the desiccant, drying it without much added complexity.

Tests would need to be done in order to find a range of H_2O_2 concentration and relative saturation that results in successful decontamination. This would give us a safety factor on acceptable operating parameters, and allow better comprehension of which components could be used.

Cycle control is currently manual, and depends on initial saturation, dryer performance and vaporizer performance. To attain ease of use comparable to commercial systems, some work needs to be done on cycle control. It is currently manually controlled, through relatively expensive lab equipment. Using less expensive and more widely available control hardware is the next logical step for this project. Moreover, development of automated software using a non-proprietary language would allow better plug-and-play capabilities, necessary for such a system.

6.3 Future Research

Many improvements can still be made to the decontamination system and the accompanying methods and protocols to render them more practical, affordable and reliable.

First of all, there are still some aspects of the system which are not completely understood and that require more research to properly assess systemic behaviours that can possibly be modified to raise efficiency further. The Leidenfrost effect was found to have a profound effect on the evaporation time of the liquid solution, drastically slowing evaporation above a certain surface temperature. This effect is quite complex and dependant on many parameters such as surface material, surface treatment, choice of liquid, droplet size and impact velocity. It has not been properly studied for the water-hydrogen peroxide binary mixture, and there is important research that can be done to assess the Leidenfrost effect on this mixture. Potential applications include any industry where a large heat transfer occurs to an aqueous solution of hydrogen peroxide, such as flash vaporization in decontamination systems, industrial cleaning processes and rocket engines. In our case, raising the Leidenfrost temperature would permit faster vaporization, giving potentially higher evaporation efficiency. Another fluid mechanics

problem that needs attention is the ejection of macroscopic droplets during vaporization, even below the Leidenfrost temperature. These ejected droplets are not converted to gas and do not contribute towards raising the gaseous concentration, therefore lowering efficiency.

A major improvement to the work done in this project would be to assemble a list of parts with well defined specifications for each component. Ideally, these parts would be available globally at a competitive price point. This would facilitate the construction of the decontamination system in cases where local components are not available, and would give further insights on what specifications are required to obtain the desired performance.

To complement this list of parts, a control and monitoring software would need to be developed using an open-source language compatible with the aforementioned hardware list. Systems could then be deployed in a quicker manner, since little to no software tinkering would be required to operate it. A wider range of personnel could also operate the system, since no programming knowledge would be necessary.

A complete characterization of the decontamination cycle's effect on equipment still needs to be done in order to not only have such a system approved by health authorities, but also to truly compare it to commercial alternatives. For example, N95 respirators would need to be tested many times in order to determine their maximum number of decontamination cycles, as well as how fit factor and filter efficiency are affected by each cycle.

Lastly, an shoebox-sized enclosure could be designed to contain all components of the system, except for the decontamination enclosure itself. It would feature spots to place each component, with a margin to accommodate the different components in the hardware list. This enclosure could be 3D printed and therefore be highly customizable, and available wherever 3D printers are in close proximity. Given the wide spread of 3D printers, this would be an easy and inexpensive part to acquire. Once all components are assembled into this enclosure, and the open-source software loaded in the control hardware, it would only need to be deposited in a large airtight enclosure with the equipment to be processed.

REFERENCES

- [1] H. Kelly, “The classical definition of a pandemic is not elusive,” *Bulletin of the World Health Organization*, vol. 89, no. 7, pp. 540–541, jul 2011. [Online]. Available: <http://www.who.int/bulletin/volumes/89/7/11-088815.pdf>
- [2] M. S. Rosenwald. (2020) History’s deadliest pandemics, from ancient Rome to modern America. Accessed 2022-03-08. [Online]. Available: <https://www.washingtonpost.com/graphics/2020/local/retropolis/coronavirus-deadliest-pandemics/>
- [3] S. Roychoudhury *et al.*, “Viral pandemics of the last four decades: Pathophysiology, health impacts and perspectives,” *International Journal of Environmental Research and Public Health*, vol. 17, no. 24, pp. 1–39, 2020.
- [4] A. McMichael, A. J., Scheraga, J. D., Woodward, A., Corvalan, C. F., Ebi, K. L., Campbell-Lendrum, D. H., Githeko, “Climate Change and Human Health - Risks and Responses SUMMARY,” World Health Organization (WHO), Tech. Rep., 2003. [Online]. Available: <https://apps.who.int/iris/bitstream/handle/10665/42749/9241590815.pdf>
- [5] N. Spervovasilis *et al.*, “Epidemics and pandemics: Is human overpopulation the elephant in the room?” *Ethics, Medicine and Public Health*, vol. 19, p. 100728, 2021. [Online]. Available: <https://doi.org/10.1016/j.jemep.2021.100728>
- [6] M. A. B. Lucien *et al.*, “Antibiotics and antimicrobial resistance in the COVID-19 era: Perspective from resource-limited settings,” *International Journal of Infectious Diseases*, vol. 104, no. 52, pp. 250–254, 2021.
- [7] J. Cohen, “Do three new studies add up to proof of COVID-19’s origin in a Wuhan animal market?” 2022. [Online]. Available: <https://www.science.org/content/article/do-three-new-studies-add-proof-covid-19-s-origin-wuhan-animal-market>
- [8] M. Ciotti *et al.*, “The COVID-19 pandemic,” *Critical Reviews in Clinical Laboratory Sciences*, vol. 57, no. 6, pp. 365–388, 2020. [Online]. Available: <https://doi.org/10.1080/10408363.2020.1783198>
- [9] N. Phillips, “The coronavirus is here to stay - here’s what that means,” *Nature*, vol. 590, no. 7846, pp. 382–384, 2021.
- [10] COVID Live - Coronavirus Statistics - Worldometer. Accessed 2022-03-09. [Online]. Available: <https://www.worldometers.info/coronavirus/>

- [11] J. Elflein, “COVID-19 testing rate by country,” Statista, 2022. [Online]. Available: <https://www.statista.com/statistics/1104645/covid19-testing-rate-select-countries-worldwide/>
- [12] CDC, “Estimated covid-19 burden,” Feb. 2020. [Online]. Available: <https://www.cdc.gov/coronavirus/2019-ncov/cases-updates/burden.html>
- [13] A. D. Iuliano *et al.*, “Estimating under-recognized COVID-19 deaths, United States, march 2020-may 2021 using an excess mortality modelling approach,” *The Lancet Regional Health - Americas*, vol. 1, p. 100019, 2021. [Online]. Available: <https://doi.org/10.1016/j.lana.2021.100019>
- [14] H. Reese *et al.*, “Estimated Incidence of Coronavirus Disease 2019 (COVID-19) Illness and Hospitalization - United States, February-September 2020,” *Clinical Infectious Diseases*, vol. 72, no. 12, pp. E1010–E1017, 2021.
- [15] Global Change Data Lab. COVID-19 Data Explorer. Accessed 2022-03-09. [Online]. Available: <https://ourworldindata.org/coronavirus-data-explorer>
- [16] CDC, “Coronavirus Disease 2019 (COVID-19),” Feb. 2020. [Online]. Available: <https://www.cdc.gov/coronavirus/2019-ncov/science/science-briefs/underlying-evidence-table.html>
- [17] W. Cao *et al.*, “Important factors affecting COVID-19 transmission and fatality in metropolises,” *Public Health*, vol. 190, no. January, pp. e21–e23, 2021.
- [18] T. Pilishvili *et al.*, “Effectiveness of mRNA Covid-19 Vaccine among U.S. Health Care Personnel,” *New England Journal of Medicine*, vol. 385, no. 25, p. e90, 2021.
- [19] N. Andrews *et al.*, “Covid-19 Vaccine Effectiveness against the Omicron (B.1.1.529) Variant,” *New England Journal of Medicine*, pp. 1–15, 2022.
- [20] A. Dua *et al.*, “Us small-business recovery after the covid-19 crisis | McKinsey,” 2020. [Online]. Available: <https://www.mckinsey.com/industries/public-and-social-sector/our-insights/us-small-business-recovery-after-the-covid-19-crisis>
- [21] S. Helper and E. Soltas, “Why the Pandemic Has Disrupted Supply Chains,” 2021. [Online]. Available: <https://www.whitehouse.gov/cea/written-materials/2021/06/17/why-the-pandemic-has-disrupted-supply-chains/>

- [22] J. Cohen and Y. v. d. M. Rodgers, “Contributing factors to personal protective equipment shortages during the COVID-19 pandemic,” *Preventive Medicine*, vol. 141, no. September, p. 106263, 2020. [Online]. Available: <https://doi.org/10.1016/j.ypmed.2020.106263>
- [23] L. Gamio and P. S. Goodman, “How the Supply Chain Crisis Unfolded,” *The New York Times*, Dec. 2021. [Online]. Available: <https://www.nytimes.com/interactive/2021/12/05/business/economy/supply-chain.html>
- [24] Y. Wang, Z. Deng, and D. Shi, “How effective is a mask in preventing COVID-19 infection?” *MEDICAL DEVICES & SENSORS*, vol. 4, no. 1, pp. 1–12, feb 2021. [Online]. Available: <https://onlinelibrary.wiley.com/doi/10.1002/mds3.10163>
- [25] A. Jacobs, M. Richtel, and M. Baker, “‘At War With No Ammo’: Doctors Say Shortage of Protective Gear Is Dire,” *The New York Times*, Mar. 2020. [Online]. Available: <https://www.nytimes.com/2020/03/19/health/coronavirus-masks-shortage.html>
- [26] M. L. Ranney, V. Griffeth, and A. K. Jha, “Critical Supply Shortages — The Need for Ventilators and Personal Protective Equipment during the Covid-19 Pandemic,” *New England Journal of Medicine*, vol. 382, no. 18, p. e41, apr 2020. [Online]. Available: <http://www.nejm.org/doi/10.1056/NEJMp2006141>
- [27] Y. Noguchi, “Why N95 Masks Are Still In Short Supply In The U.S.” *NPR*, Jan. 2021. [Online]. Available: <https://www.npr.org/sections/health-shots/2021/01/27/960336778/why-n95-masks-are-still-in-short-supply-in-the-u-s>
- [28] CDC, “Strategies for optimizing the supply of n95 respirators,” Feb. 2020. [Online]. Available: <https://www.cdc.gov/coronavirus/2019-ncov/hcp/respirators-strategy/index.html>
- [29] WHO, “Rational Use of Personal Protective Equipment for Coronavirus Disease 2019 (COVID-19) and Considerations During Severe Shortages,” World Health Organization, Tech. Rep., 2020. [Online]. Available: <https://apps.who.int/iris/handle/10665/331695>
- [30] D. J. Perkins *et al.*, “COVID-19 global pandemic planning: Decontamination and reuse processes for N95 respirators,” *Experimental Biology and Medicine*, vol. 245, no. 11, pp. 933–939, 2020.
- [31] A. Kharbat, A. Mizer, and M. Zumwalt, “Decontamination methods of personal protective equipment for repeated utilization in medical/surgical settings,” *The*

- Southwest Respiratory and Critical Care Chronicles*, vol. 8, no. 34, pp. 27–39, apr 2020. [Online]. Available: <https://pulmonarychronicles.com/index.php/pulmonarychronicles/article/view/677>
- [32] 3M, “Decontamination of 3M Filtering Facepiece Respirators, such as N95 Respirators, in the United States - Considerations,” 3M, Tech. Rep. September, 2021.
- [33] A. Kharbat *et al.*, “PPE decontamination to overcome PPE shortage in rural area during pandemic,” *Infection Prevention in Practice*, vol. 3, no. 3, p. 100145, 2021. [Online]. Available: <https://doi.org/10.1016/j.infpip.2021.100145>
- [34] C. le Roux and A. Dramowski, “Personal protective equipment (PPE) in a pandemic: Approaches to PPE preservation for South African healthcare facilities,” *South African Medical Journal*, vol. 110, no. 6, pp. 466–468, 2020.
- [35] M. Bergman, E. M. Fisher, and B. K. Heimbuch, “A Review of Decontamination Methods for Filtering Facepiece Respirators.” *Journal of the International Society for Respiratory Protection*, vol. 37, no. 2, pp. 71–86, 2020. [Online]. Available: <http://www.ncbi.nlm.nih.gov/pubmed/33268915><http://www.pubmedcentral.nih.gov/articlerender.fcgi?artid=PMC7707143>
- [36] S. Lerouge, *Non-traditional sterilization techniques for biomaterials and medical devices*. Elsevier Masson SAS., 2012. [Online]. Available: <http://dx.doi.org/10.1533/9780857096265.97>
- [37] J. Otter *et al.*, “A guide to no-touch automated room disinfection (NTD) systems,” in *Decontamination in Hospitals and Healthcare*. Elsevier, 2014, pp. 413–460. [Online]. Available: <https://linkinghub.elsevier.com/retrieve/pii/B9780857096579500175>
- [38] J. Grossman *et al.*, “Institution of a Novel Process for N95 Respirator Disinfection with Vaporized Hydrogen Peroxide in the Setting of the COVID-19 Pandemic at a Large Academic Medical Center,” *Journal of the American College of Surgeons*, vol. 231, no. 2, pp. 275–280, 2020. [Online]. Available: <https://doi.org/10.1016/j.jamcollsurg.2020.04.029>
- [39] P. A. Kenney *et al.*, “Hydrogen peroxide vapor decontamination of N95 respirators for reuse,” *Infection Control and Hospital Epidemiology*, vol. 43, no. 1, pp. 45–47, 2022.
- [40] B. Brooks, “Final Report for the Bioquell Hydrogen Peroxide Vapor (HPV) Decontamination for Reuse of N95 Respirators,” FDA Office of Counterterrorism

- and Emerging Threats, Silver Spring, Tech. Rep., 2016. [Online]. Available: <http://dx.doi.org/10.1016/j.watres.2012.03.036>
- [41] T. Y. Fu, P. Gent, and V. Kumar, “Efficacy, efficiency and safety aspects of hydrogen peroxide vapour and aerosolized hydrogen peroxide room disinfection systems,” *Journal of Hospital Infection*, vol. 80, no. 3, pp. 199–205, 2012.
- [42] P. Orlando *et al.*, “Surface disinfection: Evaluation of the efficacy of a nebulization system spraying hydrogen peroxide,” *Journal of Preventive Medicine and Hygiene*, vol. 49, no. 3, pp. 116–119, 2008.
- [43] W. Kowalski, *Ultraviolet Germicidal Irradiation Handbook*. Berlin, Heidelberg: Springer Berlin Heidelberg, 2009. [Online]. Available: <http://link.springer.com/10.1007/978-3-642-01999-9>
- [44] D. Mills *et al.*, “Ultraviolet germicidal irradiation of influenza-contaminated N95 filtering facepiece respirators,” *American Journal of Infection Control*, vol. 46, no. 7, pp. e49–e55, 2018. [Online]. Available: <https://doi.org/10.1016/j.ajic.2018.02.018>
- [45] W. G. Lindsley *et al.*, “Effects of Ultraviolet Germicidal Irradiation (UVGI) on N95 Respirator Filtration Performance and Structural Integrity,” *Journal of Occupational and Environmental Hygiene*, vol. 12, no. 8, pp. 509–517, 2015.
- [46] E. Schnell *et al.*, “Construction and validation of an ultraviolet germicidal irradiation system using locally available components,” *PLoS ONE*, vol. 16, no. July, pp. 1–14, 2021. [Online]. Available: <http://dx.doi.org/10.1371/journal.pone.0255123>
- [47] B. E. Baker and C. Ouellet, “THE THERMAL DECOMPOSITION OF HYDROGEN PEROXIDE VAPOUR,” *Canadian Journal of Research*, vol. 23b, no. 5, pp. 167–182, sep 1945. [Online]. Available: <http://www.nrcresearchpress.com/doi/10.1139/cjr45b-021>
- [48] P. Pędziwiatr *et al.*, “Decomposition of hydrogen peroxide - kinetics and review of chosen catalysts,” *Acta Innovations*, no. 26, pp. 45–52, jan 2018. [Online]. Available: <http://www.proakademia.eu/en/acta-innovations/find-issues/all-issues/all-articles/461.html>
- [49] Occupational Safety and Health Administration (OSHA), “Personal Protective Equipment - Overview | Occupational Safety and Health Administration.” [Online]. Available: <https://www.osha.gov/personal-protective-equipment>

- [50] Division of the Federal Register of The United States, “Part 84 - APPROVAL OF RESPIRATORY PROTECTIVE DEVICES,” *Code of Federal Regulations*, pp. 632–695, 1995. [Online]. Available: <https://www.ecfr.gov/current/title-42/part-84>
- [51] M. M. Bandi, “Electrocharged facepiece respirator fabrics using common materials,” *Proceedings of the Royal Society A: Mathematical, Physical and Engineering Sciences*, vol. 476, no. 2243, p. 20200469, nov 2020. [Online]. Available: <https://royalsocietypublishing.org/doi/10.1098/rspa.2020.0469>
- [52] Health Products and Food Branch Medical Devices Directorate, “Notice – Important Regulatory Considerations for the Reprocessing of Single Use N95 Respirators during the COVID-19 Response Context:,” 2020. [Online]. Available: https://www.healthcarecan.ca/wp-content/uploads/HealthCanada/NoticeReprocessingN95Respirators.pdf?utm_source=Master+List&utm_campaign=fab2ca41f3-EMAIL_CAMPAIGN_2019_03_07_07_25_COPY_01&utm_medium=email&utm_term=0_0bdb7418ff-fab2ca41f3-1266822145
- [53] Battelle, “Guide for Identifying FDA EUA Authorized N95 Respirators for Battelle CCDS TM Processing – updated July 14 , 2020 Select 3M N95 and FFR processability using Battelle CCDS TM,” Battelle, Tech. Rep., 2020. [Online]. Available: <https://www.ema.ohio.gov/Documents/covid19/BattelleCCDS.pdf>
- [54] IS MED Specialties, “Hydrogen Peroxide Material Compatibility Chart,” Englewood, CO, 2020. [Online]. Available: <https://www.industrialspec.com/images/files/hydrogen-peroxide-material-compatibility-chart-from-ism.pdf>
- [55] Steris, “MATERIAL COMPATIBILITY WITH VAPORIZED HYDROGEN PEROXIDE (VHP ®) STERILIZATION,” Steris, Tech. Rep., 2002. [Online]. Available: [http://www.sterislifesciences.com/\\$\sim\\$/media/Files/LifeSciences_com/PDF/BiodecontaminationServices/MaterialCompatibilitywithVaporizedHydrogenPeroxide.ashx](http://www.sterislifesciences.com/\sim/media/Files/LifeSciences_com/PDF/BiodecontaminationServices/MaterialCompatibilitywithVaporizedHydrogenPeroxide.ashx)
- [56] NIOSH, “Decontaminated Assessment Results | NPPTL | NIOSH | CDC,” Apr. 2021. [Online]. Available: <https://www.cdc.gov/niosh/npptl/respirators/testing/DeconResults.html>
- [57] E. Linley *et al.*, “Use of hydrogen peroxide as a biocide: New consideration of its mechanisms of biocidal action,” *Journal of Antimicrobial Chemotherapy*, vol. 67, no. 7, pp. 1589–1596, 2012.

- [58] M. E. Falagas *et al.*, “Airborne hydrogen peroxide for disinfection of the hospital environment and infection control: A systematic review,” *Journal of Hospital Infection*, vol. 78, no. 3, pp. 171–177, 2011. [Online]. Available: <http://dx.doi.org/10.1016/j.jhin.2010.12.006>
- [59] M. F. Baker Jr. *et al.*, “System and method for vaporized hydrogen peroxide cleaning of an incubation chamber,” United States of America Patent US 10 738 271 B2, 2020.
- [60] R. Pohanish, *Sittig’s Handbook of Toxic and Hazardous Chemicals and Carcinogens*, 6th ed. Norwich, NY : William Andrew, 2012.
- [61] C. Hultman, A. Hill, and G. McDonnell, “The physical chemistry of decontamination with gaseous hydrogen peroxide,” *Pharmaceutical Engineering*, vol. 27, no. 1, pp. 22–32, 2007.
- [62] C. F. Yen *et al.*, “Assessing changes to N95 respirator filtration efficiency, qualitative and quantitative fit, and seal check with repeated vaporized hydrogen peroxide (VHP) decontamination,” *American Journal of Infection Control*, vol. 50, no. 2, pp. 217–219, 2022. [Online]. Available: <https://doi.org/10.1016/j.ajic.2021.11.005>
- [63] S. Dufresne and T. Richards, “The first dual-sterilant low-temperature sterilization system,” *Canadian Journal of Infection Control*, vol. 31, no. 3, pp. 169–174, 2016.
- [64] A. Schwartz *et al.*, “Decontamination and Reuse of N95 Respirators with Hydrogen Peroxide Vapor to Address Worldwide Personal Protective Equipment Shortages During the SARS-CoV-2 (COVID-19) Pandemic,” *Applied Biosafety*, vol. 25, no. 2, pp. 67–70, 2020.
- [65] N95Decon, “Technical Report for H2O2-Based N95 Reuse Risk Management,” 2020. [Online]. Available: https://static1.squarespace.com/static/5e8126f89327941b9453eeef/t/5ea25d8146c37a5e245b2020/1587699073860/2020-04-23_N95DECON_HydrogenPeroxide_Technical_Report_v2.0_final.pdf
- [66] D. Rempel *et al.*, “Hydrogen Peroxide Methods for Decontaminating N95 Filtering Facepiece Respirators,” *Applied Biosafety*, vol. 26, no. 2, pp. 71–79, 2021.
- [67] Natural Resources Canada, “Chemicals of Concern - Regulating the Sale of Restricted Components,” Jun. 2011, last Modified: 2020-06-30 Publisher: Natural Resources Canada. [Online]. Available: <https://www.nrcan.gc.ca/our-natural-resources/minerals-mining/mining/explosive-regulations/chemicals-concern-regulating-sale-restricted-components/9957>

- [68] D. Watling *et al.*, “Theoretical analysis of the condensation of hydrogen peroxide gas and water vapour as used in surface decontamination,” *PDA Journal of Pharmaceutical Science and Technology*, vol. 56, no. 6, pp. 291–299, 2002.
- [69] W. Haynes, *CRC Handbook of Chemistry and Physics*, 95th ed., W. M. Haynes, Ed. Hoboken, 2014.
- [70] P. A. Giguère *et al.*, “HYDROGEN PEROXIDE AND ITS ANALOGUES: VII. CALORIMETRIC PROPERTIES OF THE SYSTEMS H₂O – H₂O₂ AND D₂O – D₂O₂,” *Canadian Journal of Chemistry*, vol. 33, no. 5, pp. 804–820, may 1955. [Online]. Available: <http://www.nrcresearchpress.com/doi/10.1139/v55-063>
- [71] M. Chase, *NIST-JANAF Thermochemical Tables, 4th Edition*. American Institute of Physics, -1, 1998-08-01 1998.
- [72] S. S.Zumdall, “Water - Physical properties | Britannica.” [Online]. Available: <https://www.britannica.com/science/water/Physical-properties>
- [73] PubChem, “Hydrogen peroxide.” [Online]. Available: <https://pubchem.ncbi.nlm.nih.gov/compound/784>
- [74] P. A. Giguère and I. D. Liu, “KINETICS OF THE THERMAL DECOMPOSITION OF HYDROGEN PEROXIDE VAPOR,” *Canadian Journal of Chemistry*, vol. 35, no. 4, pp. 283–293, apr 1957. [Online]. Available: <http://www.nrcresearchpress.com/doi/10.1139/v57-042>
- [75] P. A. Giguère, “THE THERMAL DECOMPOSITION OF HYDROGEN PEROXIDE VAPOUR. II.” *Canadian Journal of Research*, vol. 25b, no. 2, pp. 135–150, mar 1947. [Online]. Available: <http://www.nrcresearchpress.com/doi/10.1139/cjr47b-018>
- [76] S. Makjan *et al.*, “Effects of hydrogen peroxide on 304 stainless steel in high temperature water,” *Journal of Physics: Conference Series*, vol. 1380, no. 1, pp. 3–7, 2019.
- [77] E. Y. Yazici and H. Deveci, “Factors Affecting Decomposition of Hydrogen Peroxide,” *Proceedings of the XIIth international mineral processing symposium*, no. June 2014, pp. 609–616, 2010.
- [78] Z. B. Jildeh *et al.*, “Development of an in-line evaporation unit for the production of gas mixtures containing hydrogen peroxide – numerical modeling and experimental results,” *International Journal of Heat and Mass Transfer*, vol. 143, p. 118519, 2019. [Online]. Available: <https://doi.org/10.1016/j.ijheatmasstransfer.2019.118519>

- [79] J. Spiegelman and D. Alvarez, "Cheating Raoult's Law to Enable Delivery of Hydrogen Peroxide as a Stable Vapor," *Gases & Instrumentation*, vol. January/Fe, no. February, pp. 14–19, 2015. [Online]. Available: <http://www.rasirc.com/resources/articles/article-Cheating-Raoults-Law-Stabilized-Hydrogen-Peroxide-Vapor.pdf>
- [80] T. Coles and S. Lehtinen, "Real-time optimisation of vapour phase hydrogen peroxide bio-decontamination cycles using a new combined sensor," *Clean Air and Containment Review*, no. 43, pp. 4–5, 2020. [Online]. Available: <https://www.vaisala.com/sites/default/files/documents/CACR-Realtime-optimisation-vapour-phase-hydrogen-peroxide-biodecontamination-new-combined-sensor.pdf>
- [81] S. Lehtinen, "Understanding Critical Measurement Parameters in Vaporized Hydrogen Peroxide Bio-decontamination," *Clean Air and Containment Review*, no. 41, pp. 6–8, 2020.
- [82] Vaisala, "H2O2 Conversions - FORMULAS AND METHODS FOR CALCULATING VAPORIZED HYDROGEN PEROXIDE PARAMETERS," pp. 1–14, 2020.
- [83] D. Quéré, "Leidenfrost Dynamics," *Annual Review of Fluid Mechanics*, vol. 45, no. 1, pp. 197–215, 2013. [Online]. Available: <https://www.annualreviews.org/doi/10.1146/annurev-fluid-011212-140709>
- [84] J. J. Valencia and P. N. Quested, "Thermophysical properties," *ASM*, vol. 15, pp. 468–481, 2008.
- [85] M. Finnegan *et al.*, "Mode of action of hydrogen peroxide and other oxidizing agents: differences between liquid and gas forms," *Journal of Antimicrobial Chemotherapy*, vol. 65, no. 10, pp. 2108–2115, oct 2010. [Online]. Available: <https://academic.oup.com/jac/article-lookup/doi/10.1093/jac/dkq308>
- [86] R. J. Fischer *et al.*, "Effectiveness of N95 respirator decontamination and reuse against SARS-CoV-2 Virus," *Emerging Infectious Diseases*, vol. 26, no. 9, pp. 2253–2255, 2020.
- [87] S. S. Block, "Peroxygen compounds," in *Disinfection, sterilization, and preservation*. Philadelphia: Lippincott Williams & Wilkins, 1991, pp. 185–204.

APPENDIX A ADDITIONAL TEST DATA

The data presented below is either results of various tested parameters, or examples of raw data for a given test.

Figure A.1 shows the relation between H_2O_2 injection rate and maximum concentration, obtained from tests such as those presented in figures A.2 and A.3. These 2 latter graphs show the raw data given by the LABview software, and were mostly used for peak concentration readings, and as such are not necessarily formatted to academic standards. The two curves represent the values read by the two sensors, with the ATI sensor giving the highest value. The Y-axis represents gaseous H_2O_2 concentration, while the X-axis represents time. Figure A.4 shows the relative saturation of the 0.5 ml/min test, with the Y and X axes being relative saturation and time respectively.

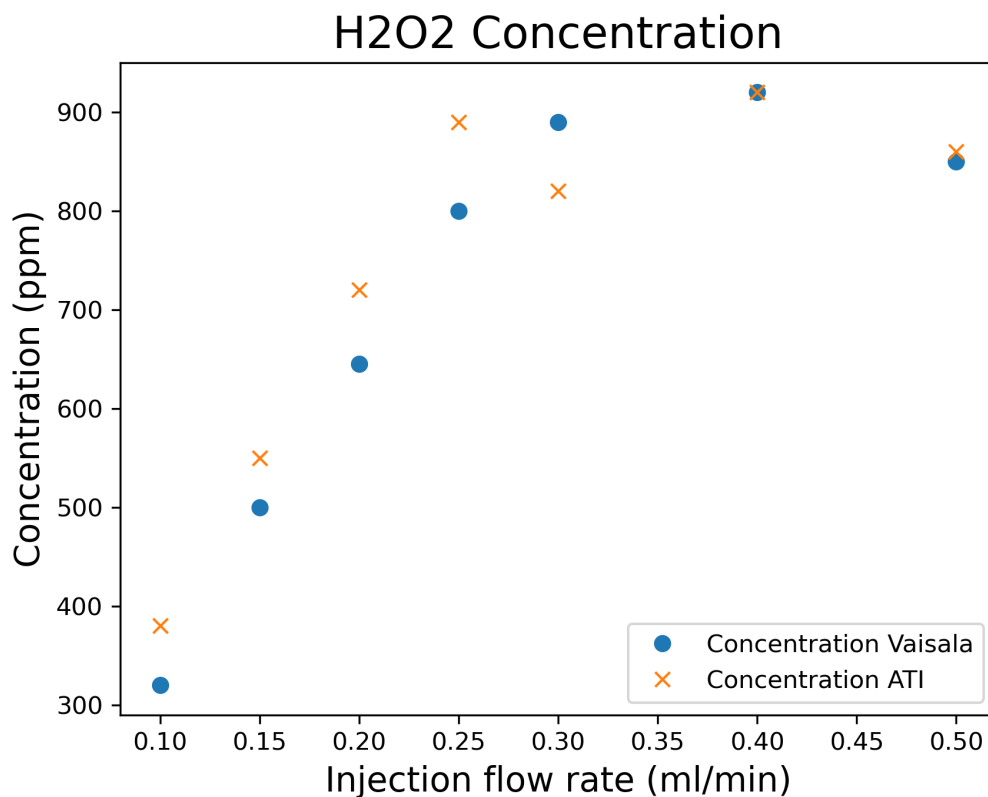


Figure A.1 Peak concentration vs. injection flow rate

The following graphs show the concentration of gaseous H_2O_2 plotted against time, with

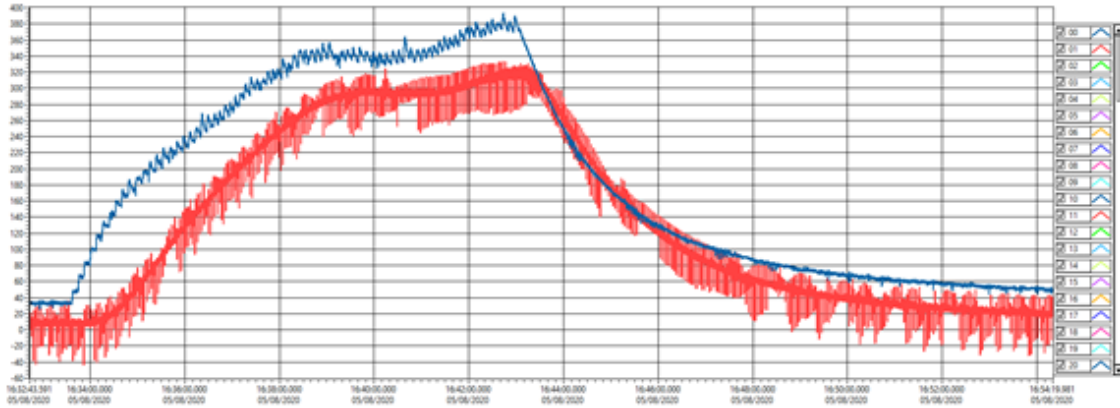


Figure A.2 Concentration vs. time at 0.1 ml/min

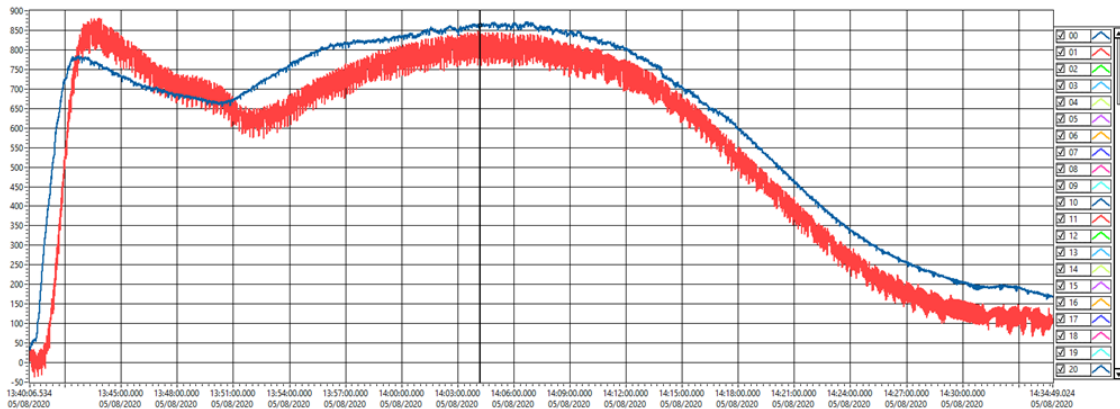


Figure A.3 Concentration vs. time at 0.5 ml/min

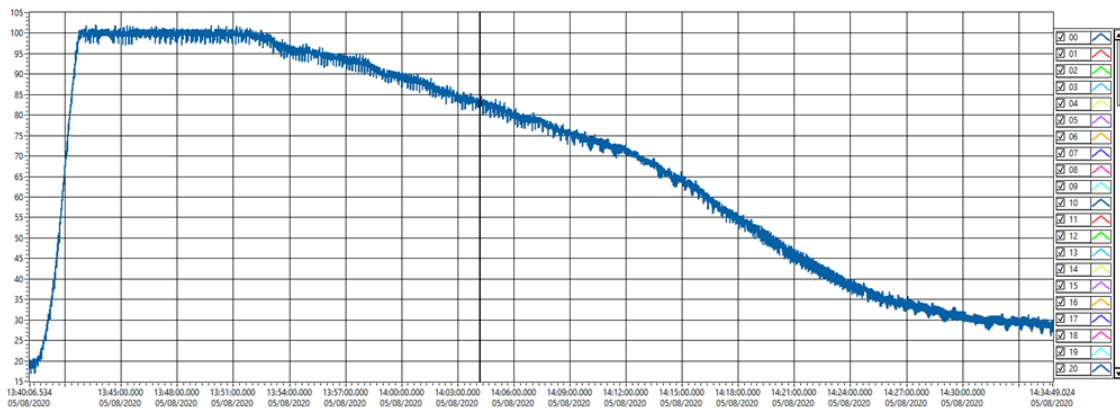


Figure A.4 Relative saturation vs. time at 0.5 ml/min

different surface area inside the enclosure. These tests were used to determine if the addition of non-reactive or low-reactive material during the test affected the maximum attainable

concentration in a significant manner, as geometry seemed to affect the vapour decomposition rate according to research done by Baker and Ouellet [47]. We used acrylic plates of constant dimensions to add surface area inside the enclosure, neatly arranged in a purpose-built 3D printed ABS mount. We found that adding such surface area did not significantly affect the concentration of H_2O_2 during the test.

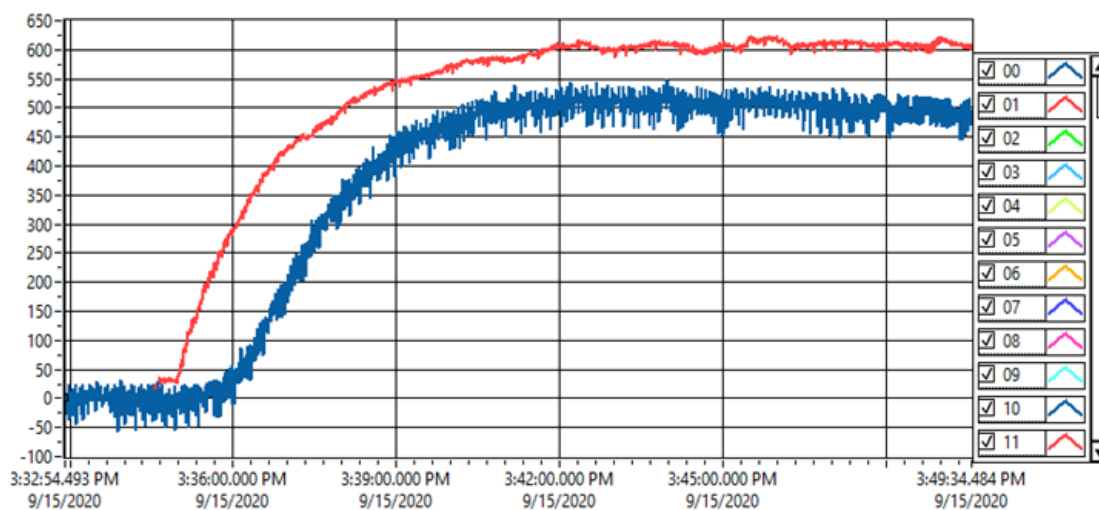


Figure A.5 Concentration vs. time with no added plates

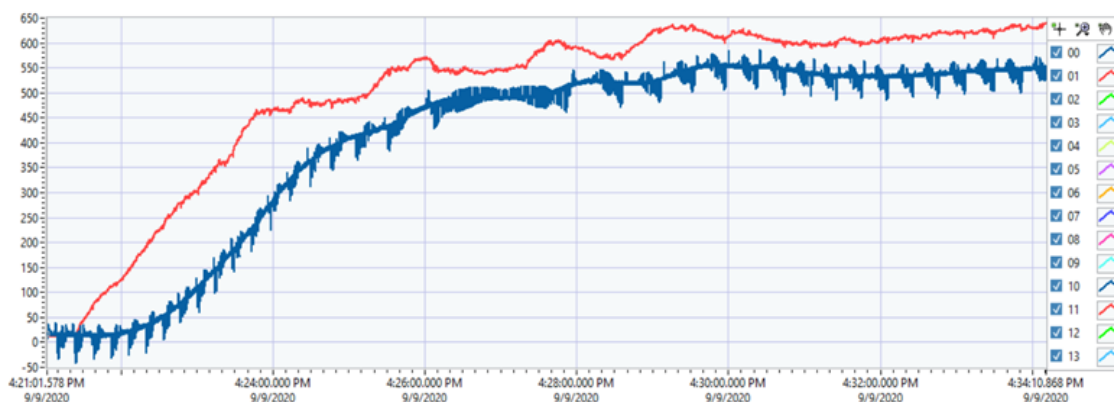


Figure A.6 Concentration vs. time with 6 added plates

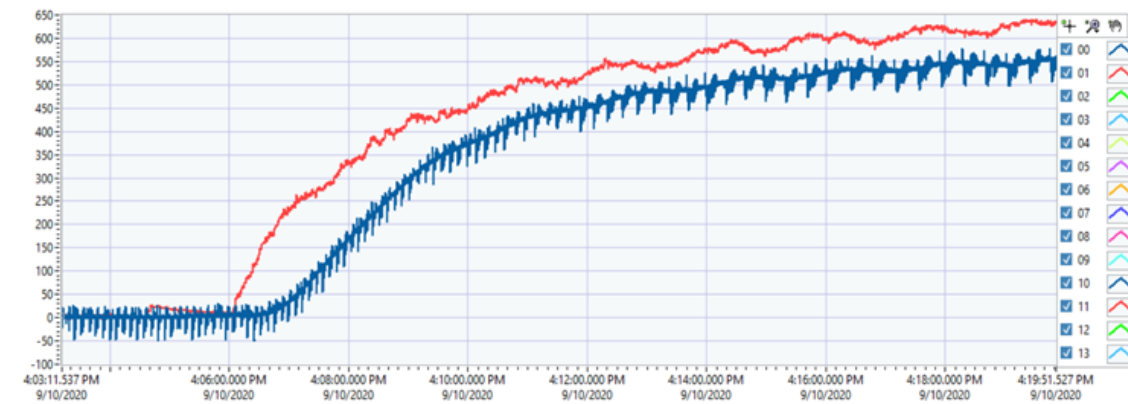


Figure A.7 Concentration vs. time with 30 added plates